Journal of Medicinal Chemistry

Article

pubs.acs.org/jmc

Development of Selective Clk1 and -4 Inhibitors for Cellular Depletion of Cancer-Relevant Proteins

Ahmed K. ElHady,[†] Mohammad Abdel-Halim,[†] Ashraf H. Abadi,[†] and Matthias Engel*[,‡]

[†]Department of Pharmaceutical Chemistry, Faculty of Pharmacy and Biotechnology, German University in Cairo, Cairo 11835, Egypt

[‡]Pharmaceutical and Medicinal Chemistry, Saarland University, Campus C2.3, D-66123 Saarbrücken, Germany

Supporting Information

ABSTRACT: In cancer cells, kinases of the Clk family control the supply of full-length, functional mRNAs coding for a variety of proteins essential to cell growth and survival. Thus, inhibition of Clks might become a novel anticancer strategy, leading to a selective depletion of cancer-relevant proteins after turnover. On the basis of a Weinreb amide hit compound, we designed and synthesized a diverse set of methoxybenzothiophene-2-carboxamides, of which the N-benzylated derivative showed enhanced Clk1 inhibitory activity. Introduction of a *m*-fluorine in the benzyl moiety eventually led to the discovery of compound **21b**, a potent inhibitor of Clk1 and -4 (IC_{50} = 7 and 2.3 nM, respectively), exhibiting an unprecedented selectivity over Dyrk1A. **21b** triggered the depletion of EGFR, HDAC1, and p70S6 kinase from the cancer cells, with potencies in line with the measured GI_{50} values. In contrast, the cellular effects of congener **21a**, which inhibited Clk1 only weakly, were substantially lower.

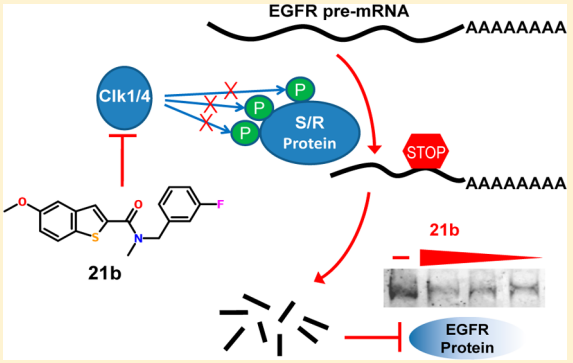

INTRODUCTION

The Clks (Cdc2-like kinases) are dual specificity protein kinases that are implicated in the regulation of pre-mRNA splicing. In the nucleus, the Clks phosphorylate serine/arginine (SR)-rich proteins, triggering the release of the latter into the nucleoplasm, where they modulate the selection of splice sites during pre-mRNA processing.[1] The Clk family consists of four highly homologous members: Clk1/STY and Clks 2−4. While Clk1, -2, and -4 are expressed in a variety of tissues, the highest levels of Clk3 protein are found in mature spermatozoa, suggesting a role in the fertilization process.[2] With respect to Clk1, -2, and -4, distinct physiological roles were barely identified so far. However, when the involvement of the Clk isoforms was probed in a pathological context, functional differences were found: e.g., overexpressed Clk1 increased the production of viral gag protein, whereas Clk2 suppressed it.[3] Compared with the other major family of SR protein kinases, the splicing-related protein kinases (SRPKs), Clks have a less constrained substrate recognition, allowing them to perform the functionally important hyperphosphorylation of splicing factors such as ASF/SF2.[4,5] Therefore, in cells with different active Clks, it can be expected that they have at least partially overlapping substrate specificities. Indeed, it was previously shown that in endothelial HUVEC cells, which express all Clk isoforms, siRNA-mediated downregulation of both Clk1 and -4 was required to decrease the generation of mature full-length tissue factor (TF) mRNA from pre-mRNA. On the other hand, the alternatively spliced TF mRNA was depleted through downregulation of either Clk1 or -4.[6] These data demonstrated that in cells expressing more than one Clk isoform, simultaneous inhibition of several Clks might be more effective in modulating particular splicing events.

Direct links between Clk1 activity and cancer growth were established, such as the multisite phosphorylation of the alternative splicing factor SPF45, which is overexpressed in cancer and stimulates cell migration and invasion through exon skipping in several target mRNAs, including Fas mRNA. Phosphorylation by Clk1 increased SPF45 protein expression, whereas inhibition of Clk1 enhanced SPF45 degradation through a proteasome-dependent pathway.[7]

Clk1 not only regulates the production of different proteins derived from splice variants but also maintains the supply of correct mRNAs coding for full-length proteins.[8] In this case, Clk1 prevents exon skipping which would lead to frameshifts and premature termination codons downstream of the junctions. Consequently, inhibition of Clk1 results in nonsense-mediated decay (NMD) of faulty mRNAs, finally leading to depletion of the corresponding proteins after cellular protein turnover. Interestingly, Araki et al. had demonstrated in a whole transcriptome analysis that the majority of genes whose splicing was affected by Clk1/2 inhibition play roles in metabolic processes and cell cycle pathways, all of which promoted cell

Special Issue: Inducing Protein Degradation as a Therapeutic Strategy

Received: January 10, 2017

DOI: 10.1021/acs.jmedchem.6b01915
J. Med. Chem. XXXX, XXX, XXX−XXX

growth and survival.[8] Recent studies provided evidence that Clk1 and also Clk4 are mediators of cell survival especially in hypoxic tumor cells.[9,10] Under hypoxic conditions, hypoxia-inducible factors (HIFs) up-regulate Clk1/4 at mRNA and protein levels. It was shown that siRNA-mediated knock-down of Clk1 decreases hypoxia-dependent full-length carbonic anhydrase IX mRNA and protein levels, and modulates the hypoxia-dependent cysteine-rich angiogenic inducer 61.[9] Although Clk4 was less well studied so far, it may have even greater importance for cancer development, as it was found, along with Clk2, to be one of the most frequently overexpressed kinases in a variety of human tumors.[11] The closely related isoenzyme Clk2 was already demonstrated to have oncogenic potential and was found amplified and overexpressed in a significant fraction of human breast tumors.[12]

Among the previously published Clk inhibitors, (1*Z*)-1-(3-ethyl-5-methoxy-2(3*H*)-benzothiazolylidene)-2-propanone (**31**), known as TG003, found widespread use as a tool compound that inhibits Clk1 and Clk4 with comparable potencies (IC_{50} reported between 15 and 49 nM in different studies).[13,14] However, **31** also inhibited nonsplicing-related kinases such as CK1δ and CK1γ2 (K_d values of 150 and 270 nM, respectively; see Figure 3 in ref 15) as well as Dyrk2 and haspin (see Table S3, Supporting Information in ref 16). The most frequently reported off-targets of Clk inhibitors, irrespective of the chemotype, are mainly Dyrk1A/1B but also haspin, STK17, CK2, and MLCK2.[17] Although Dyrk1A is also involved in the regulation of alternative splicing, another confirmed role is to counteract cardiac hypertrophy through phosphorylation of NFAT,[18] suggesting that pharmacological inhibition might implicate severe side effects. Another compound, ethyl 3-[(*E*)-2-amino-1-cyanoethenyl]-6,7-dichloro-1-methylindole-2-carboxylate (KH-CB19), while showing good overall selectivity, equally inhibited Clk1, Clk4, and Dyrk1A in the two digit nM range.[14] Further Clk/Dyrk1A co-inhibitors comprise imidazo[1,2-*b*]pyridazines[19] and benzobisthiazoles,[20] which were not tested against further typical off-target kinases. Araki et al. identified in a high-throughput screening three imidazopyridine derivatives as potent inhibitors of Clk2 and, to a lesser extent, of Clk1.[8] However, in the extended selectivity profiling, neither Clk4 nor the above-mentioned challenging off-targets were included; hence the true selectivity cannot be evaluated.

In the present study, we describe the development of new Clk1/4 inhibitors with high selectivity over Dyrk1A and other major off-target kinases. Furthermore, selective depletion of cell growth-related proteins is demonstrated following Clk inhibition in tumor cell lines.

RESULTS AND DISCUSSION

Compound Design. In a previous study, we described the development of the fragment-like hydroxybenzothiophene ketone **29**[17] from the larger ketone **28** as a Dyrk1A/Clk1 co-inhibitor (Figure 1). **29** displayed potencies in the higher nM range. Interestingly, the Weinreb amide derivative **30**[17] was also well tolerated by the Clk1 binding site. On the other hand, the modifications in **30**, also including a replacement of the free hydroxyl group by methoxy, had decreased the potency toward Dyrk1A. Hence **30** was identified as moderately selective hit for Clk1 (9-fold selectivity over Dyrk1A), with an IC_{50} of about 100 nM.[17] In order to optimize the hit compound, molecular modeling was performed based on the Clk1 cocrystal structure with hymenialdisine (PDB code 1Z57);[4] the binding model

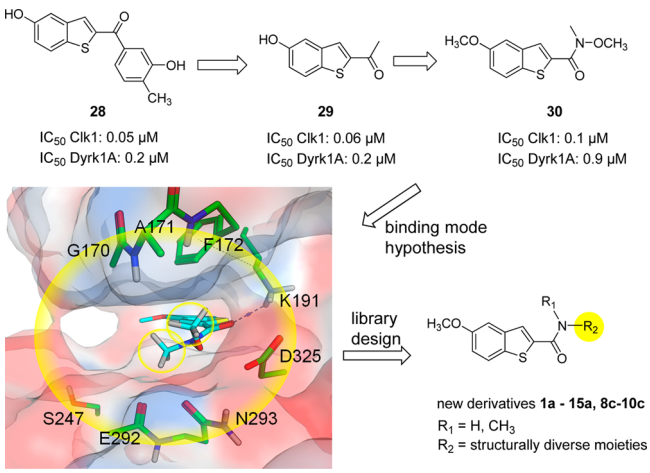

Figure 1. From previous hit compounds against Clk1 to the design of a diverse library of methoxybenzothiophene amides. Previously identified co-inhibitors of Clk1 and Dyrk1A such as **28** could be downsized to the fragment-like compound **29** without loss of potency, and the carboxamide derivative **30** was also tolerated by the Clk1 binding site.[17] A hypothetical binding model was derived, in which both *N*- and *O*-methyl groups of **30** pointed outside the ATP-binding pocket (marked by small yellow circles); thus, several H-bond donor/acceptor functions (e.g., from the peptide backbones of Ala171 and Glu292), an acidic (Asp325), and an aromatic moiety (Phe172) were all located within a 4.5 Å radius (large yellow circle), which could potentially be addressed by amide-linked molecule extensions. Following these considerations, a focused library of methoxybenzothiophene amides was designed and synthesized (see Table 1).

suggested that the ether oxygen of **30** might interact with the backbone NH of Leu244 and the amide carbonyl with the ε-amino function of Lys191 (cf. Figure 1). In the resulting binding orientation, the side chains of Phe172, Asp325, and Asn293, as well as several backbone amides, were all located within reach of the amide-linked moieties, potentially enabling a variety of interactions (Figure 1). On the basis of this model, we chose a diversification strategy for our library design, envisaging the introduction of various structural extensions at the amide function, which could establish different types of interactions (Figure 1, Table 1). This should increase the chances to improve the potency while maintaining or even enhancing the selectivity for Clks.

Chemistry. The synthesis of the methoxybenzothiophene-2-carboxamides was accomplished through a three-step synthesis (Scheme 1), where ethyl thioglycolate was reacted with 2-fluoro-5-methoxybenzaldehyde in the presence of potassium carbonate to afford the 5-methoxybenzothiophene-2-carboxylic acid ethyl ester (**1**) in good yield. After alkaline hydrolysis of the ethyl ester, the methoxybenzothiophene-2-carboxamides (**1a**–**27a**) were synthesized by direct coupling of the 5-methoxybenzothiophene-2-carboxylic acid (**2**) with different amines using HBTU in the presence of triethylamine. The N-methylation of some secondary amide derivatives was done through deprotonation using potassium bis(trimethylsilyl)-amide (KHMDS) at 0 °C, followed by trapping of the resulting anion by the addition of iodomethane (Scheme 2). An additional step of ester hydrolysis was required to deprotect the carboxyl group to prepare the amide derivatives of the glycine, L-valine and L-alanine amino acids (Scheme 3).

Biological Evaluation. When the diverse set of probe compounds was screened against human Clk1, it became clear

DOI: 10.1021/acs.jmedchem.6b01915
J. Med. Chem. XXXX, XXX, XXX−XXX

Table 1. Screening of a Diversified Library of Methoxybenzothiophene-2-carboxylamides Derivatives against Clk1

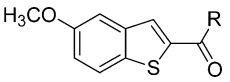

Cpd No.	R	% Inhibition at 100 nM[a]	Cpd No.	R	% Inhibition at 100 nM[a]
1a	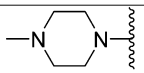	0	8c	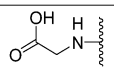	0.5
2a	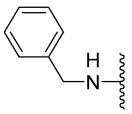	59.4 (IC_{50}: 84 ± 11 nM[b])	9c	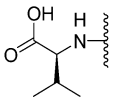	0
3a	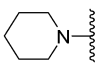	0	10a	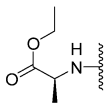	0
4a	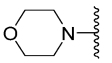	0	10c	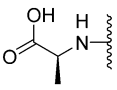	0
5a	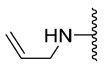	37	11a	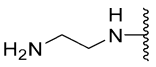	7.7
6a	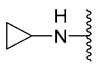	25	12a	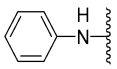	0.54
7a	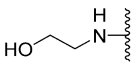	0	13a	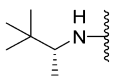	6.0
8a	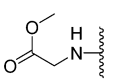	0	14a	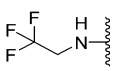	39.8
9a	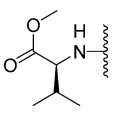	18.8	15a	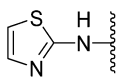	28.2

[a]Data shown are the mean of at least two independent experiments; SD ≤ 10%. [b]IC_{50} ± SD.

that hydrophobic and/or aromatic interactions rather than hydrogen (H−) bond formation enhanced the potency of the methoxybenzothiophene amides, as clearly seen with **2a**, **5a**, **6a**, **14a**, and **15a** (Table 1). With 59% inhibition at 100 nM, the benzylamide **2a** was the most potent compound of this first series; hence a small focused library of benzyl, arylmethyl, and phenylethyl amides was synthesized in the next step (Table 2). After determination of the Clk1 inhibition at 100 nM, the following general SAR could be deduced: (i) Among the homologous pairs of compounds, the one-carbon spacer between the aromatic ring and the nitrogen gave more potent analogs than the two-carbon spacer (compare **2a** and **17a**, **16a**, and **17b**; Tables 2 and 3). (ii) N-methylation of the amide greatly enhanced the inhibitory activity with all matched pairs of methylated vs unmethylated analogs (e.g., compare **2a** with **16a**, **19a** with **19b**, **23a** with **23b**, etc.). This suggested that the N-methylation increased the rotational flexibility of the amide bond by mitigating the tautomerism and/or allowing cis-configurations; it is assumed that this enabled more favorable interactions of the phenyl ring with its binding site (cf. predicted binding mode in Figure 2). (iii) Replacement of the phenyl by heterocycles generally decreased the activity (cf., **18b**, **19b**, **25a**−**27a**), suggesting that the heteroatoms did not form H-bonds but rather caused polar repulsion from the assumed binding pocket (Figure 2).

Having identified the benzylamide derivative **16a** as the most promising scaffold, we aimed at fine-tuning of the Clk1 inhibitory potency through modulation of the π-electron density. The obtained SAR indicated that this parameter strongly influenced the activity, with the electron withdrawing *m*-fluorine substitution being most advantageous. The resulting inhibitor **21b** was more potent than the unsubstituted analog **16a**, showing an IC_{50} of 7 nM (Table 3). In contrast, the analogs with electron-donating methyl (**24a**) or methoxy substituents (**23b**) exhibited a substantially reduced activity compared with **16a**. Interestingly, fluorine was only favorable in the meta-position, since the ortho- and para-regioisomers (**20b** and **22b**, respectively) were also less active than **16a**. In our binding model, the *m*-fluorophenyl ring was buried in a small, partially hydrophobic pocket in the lid of the ATP-binding site

DOI: 10.1021/acs.jmedchem.6b01915
J. Med. Chem. XXXX, XXX, XXX−XXX

Scheme 1. Synthesis of Compounds 1a−27a[a]

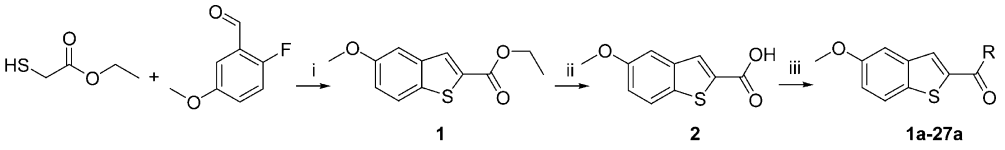

No.	R	No.	R	No.	R	No.	R
1a	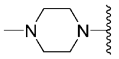	8a	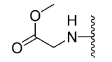	15a	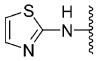	22a	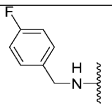
2a	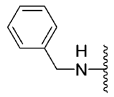	9a	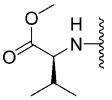	16a	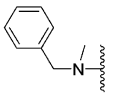	23a	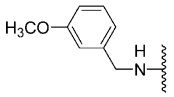
3a		10a	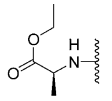	17a	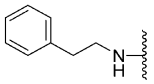	24a	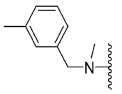
4a		11a	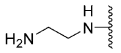	18a	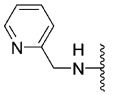	25a	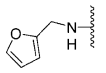
5a		12a	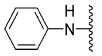	19a	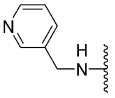	26a	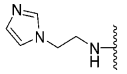
6a		13a		20a	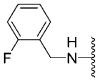	27a	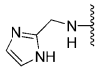
7a	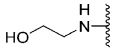	14a	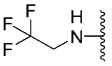	21a	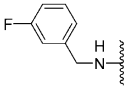		

[a]Reagents and conditions: (i) K_2CO_3 in DMF at 0 °C, 1.2 equiv of ethyl thioglyoclate, 20 min, 1 equiv of 2-fluoro-5-methoxybenzaldehyde in DMF, 70 °C, 4 h; (ii) 4 equiv of KOH in ethanol/water, 80 °C, 3 h; (iii) 2 equiv of HBTU, 4 equiv of triethylamine, 4 equiv of the appropriate amine in DCM, room temperature, overnight.

(Figure 2). While such a pocket was not induced by the type of compounds bound in the four available Clk1 cocrystal structures, it was observed before in cocrystals of the highly homologous Dyrk1A with compounds containing a branched 3-chlorobenzyl motif at the corresponding position (cf. PDB entries 2WO6 and 2VX3).[21] Due to the limited size of this pocket, the *m*-methyl (**24a**), *m*-methoxy (**23b**), but also the *p*-fluorine substituent (**22b**) would be expected to cause steric collisions (*p*-fluorine with the carbonyl of Gly173), in agreement with the markedly lower activity of these three compounds compared with the unsubstituted **16a** (cf. Table 2). Placing the fluorine in the meta-position (**21b**) apparently avoided too close contacts and moreover increased the potency 6.5-fold compared with the unsubstituted analog **16a** (Table 2). This improvement in potency might at least partially be attributed to an enhancement of hydrophobic interactions. In addition, our docking model suggested that a C−F···C═O interaction with the backbone of Glu169 might also occur. In some docking poses, the fluorine was found in a favorable position for such an orthogonal dipolar interaction (see Figure 2), with the distance (2.9 Å) and angles (∠F···C═O, 96°; ∠C−F···C, 152°) being in typical ranges found in cocrystal structures.[22] In a previous study, introduction of a single fluorine in a benzyl ring of a thrombin inhibitor led to a comparable 6-fold increase in potency owing to C−F···C═O interactions.[23]

The methyl group of **21b** was expected to induce an out-of-plane rotation of the amide group, thus favoring the biologically active conformation as predicted by the docking simulation (Figure 2). In addition, the methyl was placed in a van der Waals distance to Val324, suggesting an additional contribution to the binding affinity. Further major contributions were expected from the H-bond of the ether oxygen with Leu244, the CH−π interaction of the benzothiophene with Phe241, and the H-bond between the carbonyl and Lys191, altogether explaining the high potency of **21b** (Table 3). Overall, this binding model agreed well with the observed SAR for the Clk1 inhibitors.

Kinase Selectivity Profiling. As described in the Introduction, a quite reliable way to assess the selectivity of Clk inhibitors (apart from a full kinome scan) is to check the kinases that are supposed to be the most similar in the ATP binding pocket, which were frequently identified as off-targets in previous studies. A strong co-inhibition of Clk4 was

DOI: 10.1021/acs.jmedchem.6b01915
J. Med. Chem. XXXX, XXX, XXX−XXX

Scheme 2. Synthesis of N-Methylated Derivatives[a]

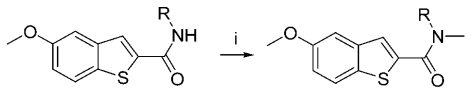

17a-23a
26a

17b-23b
26b

No.	R	No.	R
17b	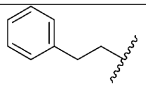	21b	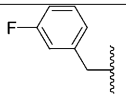
18b		22b	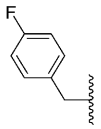
19b	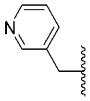	23b	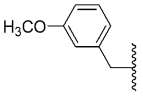
20b		26b	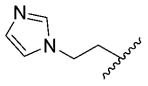

[a]Reagents and conditions: (i) 3 equiv of KHMDS, 0 °C, 1 h, 1.5 equiv of CH_3I, room temperature, 24 h.

Scheme 3. Synthesis of Carboxylic Acids 8c−10c[a]

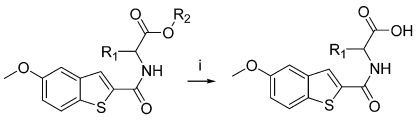

8a-10a

8c-10c

No.	R_1	Stereo-chemistry	R_2	No.	R_1	Stereo-chemistry
8a	H	……..	methyl	**8c**	H	…….
9a	isopropyl	*S*	methyl	**9c**	isopropyl	*S*
10a	methyl	*S*	ethyl	**10c**	methyl	*S*

[a]Reagents and conditions: (i) 4 equiv of KOH in ethanol/water, 80 °C, 3 h.

anticipated for our compounds **16a** and **21b** (Table 3) because Clk1 and Clk4 possess fully identical amino acid residues in and around the ATP binding pocket, suggesting that selective inhibition of either of the isoenzymes might not be possible using small molecules. Similarly, the still highly homologous Clk2 was markedly inhibited by **21b**, although with somewhat reduced potency. Our selectivity profiling revealed that the notorious off-targets haspin, STK17, and MLCK2 were not inhibited by **16a** and **21b**. The most strongly inhibited non-Clk kinases were Dyrk1A/1B; however, determination of the IC_{50} values toward Dyrk1A revealed that **16a** was still 11.5-fold selective for Clk1 (Table 3), and notably, **21b** inhibited Clk1 48.5 times and 30 times more strongly than Dyrk1A and Dyrk1B, respectively (IC_{50}: Clk1 = 6.9 nM; Dyrk1A and Dyrk1B = 340 nM and 206 nM, respectively). Thus, compound **21b** turned out to be one of the most selective Clk1/4 inhibitors described to date, with somewhat weaker effect on Clk2 as well.

How is the selectivity over Dyrk1A achieved? It is likely that the methoxy group in the 5-position of the benzothiophene forms a markedly stronger H-bond with the hinge region of Clk1 than of Dyrk1A. In our previous benzothiophene ketone series, a free 5-hydroxy group was necessary for potent inhibition of Dyrk1A, whereas the corresponding methoxy derivative was inactive.[17] Similarly, the hydroxyl derivative of the benzothiazoylidene-2-propanone **31**, termed "INDY", was 3-fold more potent toward Dyrk1A than **31** itself.[24] Molecular docking of **21b** in the Dyrk1A crystal structure from PDB entry 2W06[21] also supported this notion, since no H-bond between the NH of Leu241 (corresponding to Leu244 in Clk1) and the 5-methoxy was formed using the same docking conditions as for Clk1 (Supporting Information, Figure S1).

Inhibition of Tumor Cell Growth. In previous studies, important anticancer effects of Clk inhibitors were shown to be mediated through the modulation of pre-mRNA splicing, which in several cases led to NMD of the mRNAs of genes important for cell growth and survival.[8,9] Thus, treatment of cancer cells by Clk1/4 inhibitors cuts off the supply of intact mRNA, triggering the disappearance of the affected proteins depending on their cellular half-life.

First, we determined the potency of our best Clk1/4 inhibitors to inhibit the growth of different cancer cell lines. To this end, we selected five human cell lines of different tissue origin which differed in the expression levels of Clk1 mRNA as published in the Expression Atlas database (https://www.ebi.ac.uk/gxa/home): two cell lines with low expression (T47D (breast carcinoma) and THP-1 (monocytic leukemia)) and three cell lines with higher Clk1 expression (T24 (urinary bladder carcinoma), MDA-MB-231 (breast adenocarcinoma), and HepG2 (hepatocellular carcinoma)). Hence, a differential sensitivity toward the Clk1/4 inhibitors was expected. As shown in Table 4, the sensitivity of the cell lines toward the most potent compounds **21b** and **16a** varied, with T24 and HepG2 cells being most responsive (GI_{50} for **21b**: 0.63 μM and 2.8 μM, respectively). Intriguingly, these two cell lines also exhibited the highest mRNA and protein expression levels of Clk1. In contrast, both THP-1 and T47D were considerably less sensitive toward our inhibitors, which correlated with lower mRNA and protein expression levels of Clk1. In line with this relationship, the MDA-MB-231 cell line showed moderate sensitivity toward **21b** and intermediate Clk1 expression (Table 4). Altogether, our results suggested that enhanced Clk1 expression may indicate a stronger dependence of tumor cell growth and survival on this kinase, translating into higher sensitivity toward chemical Clk1 inhibition. In further support of this notion, the efficacy of the chosen compound series **21b**, **21a**, **16a**, and **19b** to suppress cell growth of a specific cell line correlated with their relative potency against Clk1 (cf. T24 and MDA-MB-231 cells, Table 4), suggesting that the compounds act through inhibition of Clk1/4 rather than by another mechanism.

Lack of Cytotoxicity against Nontumor Cells. In order to assess the potential therapeutic window of our Clk1/4 inhibitors, we performed a cytotoxicity assay using normal peripheral blood lymphocytes (PBLs) and human embryonic kidney cells (HEK293). Neither **21b** nor the second most potent congener **16a** showed a significant cytotoxicity toward the nonproliferating PBLs and the proliferating HEK293 cells (Table 5). This result suggested that in nontumor cells, the

DOI: 10.1021/acs.jmedchem.6b01915
J. Med. Chem. XXXX, XXX, XXX−XXX

Table 2. Inhibition of Clk1 by the Optimized Series of Methoxybenzothiophene-2-carboxylamides

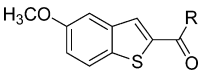

Cpd No.	R	% Inhibition at 100 nM[a]	IC_{50} (nM)[b]	Cpd. No.	R	% Inhibition at 100 nM[a]	IC_{50} (nM)[b]
16a		70.6	45 ± 6	21b	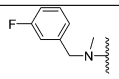	80	6.9 ± 0.12
17a	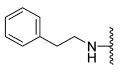	50.7	107 ± 4.9	22a	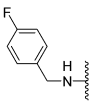	23.5	n.d.
17b	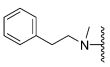	32.9	n.d.	22b		28.7	n.d.
18a		0	n.d.	23a	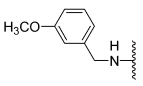	13.4	n.d.
18b		34.6	n.d.	23b	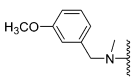	31.6	n.d.
19a		28.9	n.d.	24a		25.9	n.d.
19b		51.0	81.6 ± 2.5	25a		33.4	n.d.
20a	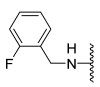	23.2	n.d.	26a	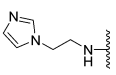	0	n.d.
20b		43.2	n.d.	26b	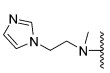	9.4	n.d.
21a	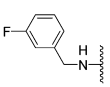	33.9	n.d.	27a		0	n.d.

[a]Data shown are the mean of at least two independent experiments; SD ≤ 10%. [b]IC_{50} ± SD; n.d., not determined.

activity of the Clk1 and -4 isoforms might not be essential to ensure cell viability and/or proliferation.

Selective Depletion of Cancer-Relevant Proteins. Next, we analyzed the effect of **21b** on the levels of selected cancer-associated proteins in the three most sensitive tumor cell lines (cf. Table 4); again, the substantially less active congener **21a** served as a control. After treatment of T24 cells with different concentrations of **21b**, the protein levels of EGFR and HDAC1 were significantly diminished in a concentration-dependent manner (Table 6, Figure 3A). A significant reduction of EGFR protein was already observed at 1.25 μM (IC_{50} = 2.2 μM, Table 4), which was in a good agreement with the observed GI_{50}. Notably, the other analyzed proteins, p70S6K, PARP-1, ERK2, CD44, PCNA, and GRP94, were not influenced (exemplarily shown are the CD44 signals). The control compound **21a**, which was much less potent against recombinant Clk1 (see Table 2) and did not reach the GI_{50} at the highest concentration tested (40 μM), showed a substantially weaker effect on the protein levels of both EGFR and HDAC1 (Figure 3A, Table 6). With the less sensitive cell line MDA-MB-231, higher concentrations of **21b** were needed to decrease protein levels (cf. IC_{50} values in Table 4); in this case it concerned EGFR and, surprisingly, not HDAC1 but S6K. However, the IC_{50} for S6K reduction in the MDA-MB-231 cells was not reached at the highest concentration of **21b** (20 μM). Again, all other proteins in the analyzed panel remained unchanged, with respect to amount and size. Thus, in both T24 and MDA-MB-231 cells, the effect of **21b** on EGFR might be a major reason for the suppression of cell growth because the IC_{50} values for EGFR depletion were in good agreement with the respective GI_{50} values. In the light of this finding, it was interesting to analyze the effects of **21b** in the HepG2 cells, which lack a strong expression of EGFR.[25] Indeed, we could not detect any EGFR protein signals in this cell line, indicating a rather low expression. On the other hand, although there was a 44% reduction of both HDAC1 and S6K protein levels at 20 μM **21b**, the main target of the Clk1/4-triggered protein depletion was not found within the analyzed set of proteins (Figure S2, Supporting Information). Thus, in cell lines that overexpress EGFR, the selective depletion of EGFR is likely a major

DOI: 10.1021/acs.jmedchem.6b01915
J. Med. Chem. XXXX, XXX, XXX−XXX

Table 3. Selectivity Profiling of Compounds 16a and 21b

	% inhibition at 1 μM[a] (IC_{50} ± SD)[b]	
kinase	16a	21b
DYRK1A	54 (520 ± 28.3 nM)	72 (340 ± 21.2 nM)
DYRK1B	58	77 (206 ± 10 nM)
DYRK3	n.i.	n.i.
DYRK4	n.i.	n.i.
Clk1	81 (45 ± 6 nM)	92 (7 ± 0.12 nM)
Clk2	73	86 (19.1 ± 0.5 nM)
Clk3	44	58
Clk4	101	101 (2.3 ± 0.24 nM)
Haspin	12	12
MLCK2	n.i.	n.i.
STK17A	23	32
SRPK1	4	2
SRPK2	10	7
CK2	n.d.	1.4

[a]The screening list was especially composed to include all kinases that were frequently reported as off-targets for diverse chemical classes of Dyrk inhibitors.[17,27,29−32] Screenings were performed as a service at Thermo Fisher Scientific at an ATP concentration of 100 μM. n.i., no inhibition. n.d., not determined. Data represent mean values of duplicates that differed by less than 7%. [b]IC_{50} values were determined mainly for **21b** for inhibition values of >50% in the primary screening. ATP concentration was 15 μM.

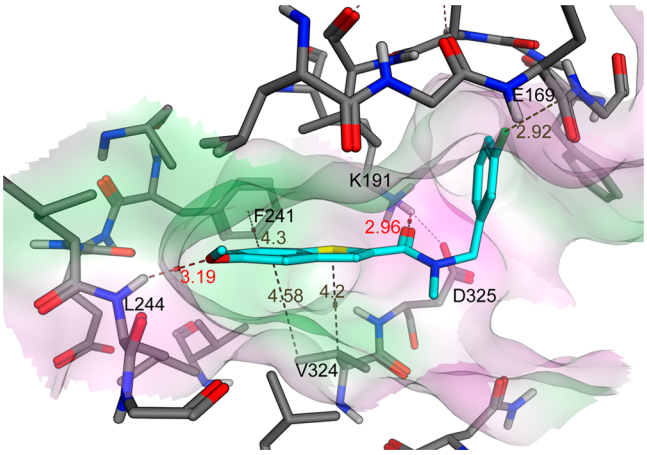

Figure 2. Model for the hypothetical interaction of **21b** with Clk1 as supported by the SAR. **21b** (cyan) was docked into the ATP binding-pocket of Clk1 (PDB code 1Z57) using MOE. Some residues that might be important for the binding are labeled. In the binding model, **21b** is anchored between the conserved Lys191 and the hinge region residue Leu244 via two hydrogen bonds (indicated in red). In addition, two CH−π interactions involving Val324 and an edge-to-face CH−π interaction with the Phe241 benzene ring were predicted. The 3-fluorophenyl ring probably binds in a partially lipophilic pocket enframed by the glycine-rich loop, also involving an orthogonal dipolar interaction of the 3-fluorine with the Glu169 carbonyl. Interactions are indicated by dashed lines, and distances between the heavy atoms are given in Å (H-bonds, red; CH−π and orthogonal dipolar interactions, brown). In the color code of the ATP binding pocket surface, green denotes the most lipophilic and magenta the most hydrophilic areas.

mechanism through which Clk inhibitors lead to cell growth inhibition, whereas in cell lines displaying weak or no EGFR expression, the mainly affected proteins remain to be identified in future studies.

It is further noteworthy that only a fraction of the analyzed cancer-relevant proteins was actually affected in the three cell lines, which was rather unexpected given the supposed ubiquitous role of the Clk isoenzymes in the regulation of alternative splicing. It could be speculated that in a given cell line, the activities of the remaining SR protein kinases, such as SRPKs and Dyrk1A, might differentially modulate the impact of Clk inhibition on exon splicings of particular pre-mRNAs. In addition to potential modulating or compensating effects of other SR protein kinases, the selection of exon-splicing sites specifically regulated through Clks seems to be determined already at the level of the branch sequence composition and length of polypyrimidine tracts in the exons. In a recent comparative transcriptomic analysis which employed the model Clk inhibitor **31**, targeting rules for exon skipping were derived from treated skeletal muscle cells. Exons skipped after treatment by **31** were shorter, had fewer splicing factor binding sites and shorter stretches of polypyrimidine tracts than the insensitive exons.[26]

CONCLUSIONS AND PERSPECTIVES

We developed a novel series of benzylated *N*-methylbenzothiophene-2-carboxamides as potent inhibitors of Clk1/4 and, to a somewhat lower extent, of Clk2. The introduction of *m*-fluorine in the benzyl moiety was key to the discovery of compound **21b**, which exhibited previously unreported selectivity over Dyrk1A, a highly homologous kinase also involved in the regulation of alternative splicing. This is considered an important advancement since Dyrk1A inhibition was previously shown to induce cardiac hypertrophy as a deleterious side effect, related to its role in antagonizing calcineurin signaling.[18] While it might be assumed that inhibition of Clk isoforms will have detrimental effects due to the vast number of influenced splicing events, our results suggest that when selective Clk inhibitors are used, the number of modulated pre-mRNA splicings might be lower than expected. Thus, although further studies are needed that specifically address this issue, it could be speculated that the application of selective Clk inhibitors in vivo might have fewer adverse side effects than one might have anticipated. In a future potential application of Clk inhibitors for anticancer therapy, prior analysis of Clk isoenzyme overexpression might be performed to identify tumors that are particularly responsive toward Clk inhibition.

EXPERIMENTAL SECTION

Chemistry. Solvents and reagents were obtained from commercial suppliers and used as received. Melting points were determined on a Stuart SMP3 melting point apparatus. All final compounds had a percentage purity of at least 95%, and this could be verified by means of HPLC coupled with mass spectrometry. Mass spectra (HPLC−ESIMS) were obtained using a TSQ quantum (Thermo Electron Corp.) instrument prepared with a triple quadrupole mass detector (Thermo Finnigan) and an ESI source. All samples were injected using an autosampler (Surveyor, Thermo Finnigan) by an injection volume of 10 μL. The MS detection was determined using a source CID of 10 V and carried out at a spray voltage of 4.2 kV, a nitrogen sheath gas pressure of 4.0×10^5 Pa, a capillary temperature of 400 °C, a capillary voltage of 35 V, and an auxiliary gas pressure of 1.0×10^5 Pa. The stationary phase used was an RP C18 NUCLEODUR 100-3 (125 mm

DOI: 10.1021/acs.jmedchem.6b01915
J. Med. Chem. XXXX, XXX, XXX−XXX

Table 4. Correlation between Clk1 Inhibitory Potency, GI_{50} Values, and Relative Clk1 Expression Levels in Different Cancer Cell Lines

cell line	T24	MDA-MB-231	HepG2	THP-1	T47D	
Clk1 mRNA levels[a,b]	6.5	5.4	8	3.3	1	
Clk1 protein levels[a,c]	1.5	1.3	3.2	1.2	1	
compd	**GI_{50} (μM)[d]**	**GI_{50} (μM)[d]**	**GI_{50} (μM)[d]**	**GI_{50} (μM)[d]**	**GI_{50} (μM)[d]**	**Clk1 inhibition IC_{50} ± SD (nM)[e]**
21b	0.6	9.6	2.8	27.2	15.3	6.9 ± 0.12
21a	>40	>40	n.d.	n.d.	n.d.	>100
16a	2.7	24.2	3.7	>30	28.8	45 ± 6
19b	12.5	25.7	n.d.	n.d.	25.4	81.6 ± 2.5

[a]Levels relative to the expression in T47D (set = 1). [b]Data taken from the Expression Atlas Database (https://www.ebi.ac.uk/gxa/home). [c]Values obtained by densitometry (SD < 8%). [d]Data shown are the mean of at least two independent experiments, SD ≤ 12%. n.d., not determined. [e]Values taken from Table 2.

Table 5. Evaluation of Cytotoxicity of Compounds 16a and 21b against Nontumor Cells

	cell type: PBLs	cell type: HEK293
compd	LC_{50} (μM)[a]	GI_{50} (μM)[a]
21b	29.4	>30
16a	>30	>30

[a]Data shown are the mean of at least two independent experiments; SD ≤ 12%.

Table 6. Correlation between Clk1 Inhibitory Potency, Reduction of Cellular Proteins, and Relative Clk1 Expression Levels in the Cell Lines MDA-MB-231 and T24

	cell line (Clk1 rel expression levels): T24 (17)		cell line (Clk1 rel expression levels): MDA-MB-231 (14)		
	IC_{50} of protein reduction (μM)[a]				
compd	EGFR	HDAC	EGFR	S6 kinase	Clk1 IC_{50} ± SD (nM)
21b	2.2	9.5	4.2	>20	6.9 ± 0.12
21a	>15	>15	>20	>20	>100

[a]IC_{50} values were derived by densitometric quantification of the signals from the immunoblot shown in Figure 3 after normalization. The values represent an average of two independent determinations; SD ≤ 15%.

× 3 mm) column (Macherey & Nagel). The solvent system consisted of water containing 0.1% TFA (A) and 0.1% TFA in acetonitrile (B). The HPLC method used a flow rate of 400 μL/min. The percentage of B started at 5%, was increased up to 100% during 7 min, was kept at 100% for 2 min, and was flushed back to 5% in 2 min and was kept at 5% for 2 min. High resolution precise mass spectra were recorded on ThermoFisher Scientific (TF, Dreieich, Germany) Q Exactive Focus system equipped with heated electrospray ionization (HESI)-II source and Xcalibur (version 4.0.27.19) software. Before analysis external mass calibration was done according to the manufacturer's recommendations. The samples were dissolved and diluted in methanol in a concentration of 3 μM and directly injected onto the Q Exactive Focus using the integrated syringe pump. All the data analyses were done in positive ion mode using voltage scans and the data collected in continuous mode. A Bruker DRX 500 spectrometer was used to obtain the ^{1}H NMR and ^{13}C NMR spectra, and a Varian Mercury VX 300 spectrometer was used to obtain spectra for two of the final amide derivatives. The chemical shifts are referenced to the residual protonated solvent signals. The IR spectra were measured on a PerkinElmer Spectrum 100 FT-IR spectrometer, PerkinElmer, Rodgau, Germany.

General Synthetic Methods and Experimental Details for Some Key Compounds. Procedure A, Synthesis of 5-Methoxybenzo[*b*]thiophene-2-carboxylic Acid Ethyl Ester (1). To an ice cooled suspension of 7.2 g (2 equiv) of K_2CO_3 in DMF (20 mL) was added ethyl thioglycolate (31.2 mmol, 1.2 equiv). The reaction mixture was stirred for 20 min at 0 °C under nitrogen, and this was followed by the gradual addition of 2-fluoro-5-methoxybenzaldehyde (26 mmol, 1 equiv) in DMF (10 mL). The mixture was heated to reflux at 70 °C for 4 h. Afterward the suspension was cooled to room temperature and poured over 100 mL of 2 M HCl, the aqueous layer was extracted by DCM (5 × 10 mL), and the combined organic layers were thoroughly washed with water and brine, dried over anhydrous $MgSO_4$, evaporated under reduced pressure, and the resulting residue was purified by column chromatography (CC) using a solvent system of (petroleum ether/DCM 3:2), giving the pure carboxylic acid ethyl ester **1** as a yellow solid in a yield of 2.9 g (47%). ^{1}H NMR (500 MHz, DMSO-d_6) δ 8.09 (s, 1H), 7.93 (d, J = 8.9 Hz, 1H), 7.53 (d, J = 2.5 Hz, 1H), 7.17 (dd, J = 8.9, 2.6 Hz, 1H), 4.34 (q, J = 7.1 Hz, 2H), 3.82 (s, 3H), 1.32 (t, J = 7.1 Hz, 3H); ^{13}C NMR (126 MHz, DMSO-d_6) δ 161.98, 157.48, 139.64, 133.92, 133.80, 130.35, 123.75, 118.04, 107.07, 61.36, 55.33, 14.11.

Procedure B, General Procedure for Ester Hydrolysis. The ethyl/methyl ester was suspended in a mixture of 50 mL of ethanol and 25 mL of water; this was followed by the addition of 4 equiv of KOH. The mixture was heated to reflux at 80 °C for 3 h. Afterward, the solvent was removed under reduced pressure, and the resulting aqueous layer was cooled to 0 °C, followed by gradual addition of conc HCl until the pH was adjusted to 1. The aqueous layer was then extracted using DCM (5 × 50 mL), and the combined organic extracts were filtered over anhydrous $MgSO_4$ and evaporated under reduced pressure giving the carboxylic acid derivative. The product was used in the next step without further purification.

Procedure C, General Procedure for the Synthesis of 5-Methoxybenzo[*b*]thiophene-2-carboxylic Acid Amide Derivatives. 5-Methoxybenzo[*b*]thiophene-2-carboxylic acid (**2**) (0.1 g, 0.5 mmol) was dissolved in DCM (30 mL), and then 0.3 g of HBTU and 2 mL of TEA were added. The reaction mixture was stirred for 30 min. Following this, the appropriate amine (4 equiv) was added dropwise, and the reaction mixture was stirred at room temperature overnight. The solvent was evaporated under reduced pressure. The residue was partitioned between 50 mL of ethyl acetate and 20 mL of water, and then the aqueous layer was extracted with three 20 mL portions of ethyl acetate. The combined organic extracts were filtered over anhydrous $MgSO_4$, the solvent was removed under reduced pressure, and the product was purified by CC to give the 5-methoxybenzo[*b*]-thiophene-2-carboxylic acid amide derivatives in different yields.

Procedure D, General Procedure for the Synthesis of 5-Methoxybenzo[*b*]thiophene-2-carboxylic Acid Methylamide Derivatives. The respective amide derivative was dissolved in dry THF and stirred at 0 °C. This was followed by the gradual addition of 3 equiv of potassium bis(trimethylsilyl)amide (0.5 M solution in THF). The reaction mixture was left to stir for 1 h, and after that CH_3I (1.5 equiv) was added. The reaction mixture was left to stir for 24 h at room temperature, and afterward, the solvent was removed under reduced pressure, then a small amount of water was added, and extraction was carried out using DCM (5 × 30 mL). The organic layers were combined, dried over anhydrous $MgSO_4$, the solvent was removed under reduced pressure, and the product was purified by CC

DOI: 10.1021/acs.jmedchem.6b01915
J. Med. Chem. XXXX, XXX, XXX−XXX

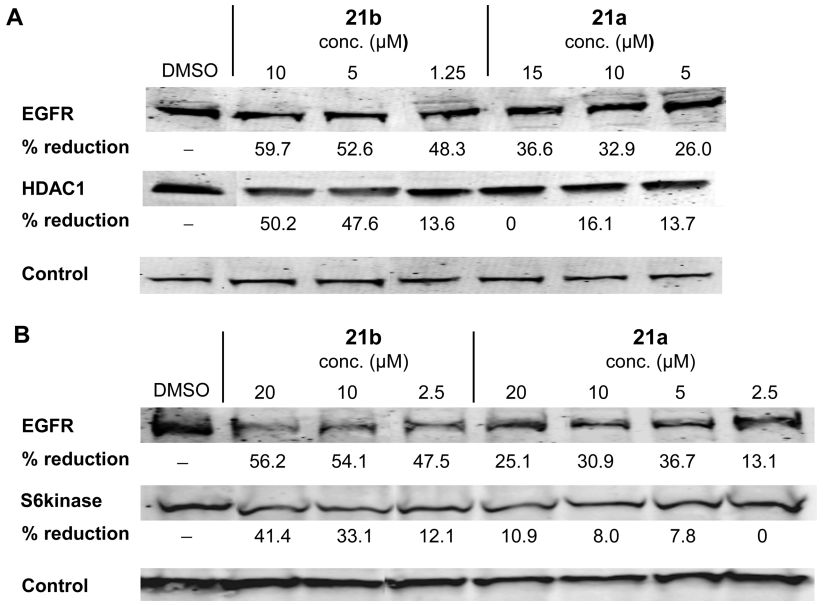

Figure 3. 21b induces cellular depletion of cancer-relevant proteins. T24 (A) and MDA-MB-231 cells (B) were treated by **21b** and the weak Clk1 inhibitor **21a** as a comparison for 3 days at the indicated concentrations. The total cellular proteins extracted from the cells were analyzed by immunoblotting using a set of antibodies directed against eight cancer-related proteins (EGFR, p70S6 kinase α, PARP-1, ERK2, HDAC1, CD44, PCNA, GRP94). Shown are the signals belonging to proteins that were significantly reduced depending on the **21b** concentrations; for comparison, one of the unchanged signal sets is also exemplarily shown (corresponding to CD44). In parts A and B, one representative result out of two separate experiments is shown.

or by salting out to give the methylated 5-methoxybenzo[*b*]thiophene-2-carboxylic acid amide derivatives in different yields.

5-Methoxybenzo[*b*]thiophene-2-carboxylic Acid (2). The compound was synthesized according to procedure B, to give a white solid in a yield of 2.3 g (90%). ^{1}H NMR (500 MHz, DMSO-d_6) δ 8.01 (d, J = 0.6 Hz, 1H), 7.91 (d, J = 8.9 Hz, 1H), 7.52 (d, J = 2.5 Hz, 1H), 7.15 (dd, J = 8.9, 2.6 Hz, 1H), 3.82 (s, 3H); ^{13}C NMR (126 MHz, DMSO-d_6) δ 163.51, 157.38, 139.84, 135.64, 133.82, 129.90, 123.73, 117.74, 106.93, 55.33.

(5-Methoxybenzo[*b*]thiophen-2-yl)(4-methylpiperazin-1-yl)-methanone(1a). The compound was synthesized according to procedure C, using 1-methylpiperazine to give a yellow solid: yield 0.05 g (31.2%). The product was purified by CC (DCM/MeOH 100:2); mp 84−85 °C; ^{1}H NMR (500 MHz, DMSO-d_6) δ 7.90 (d, J = 8.9 Hz, 1H), 7.68 (s, 1H), 7.44 (d, J = 2.5 Hz, 1H), 7.11 (dd, J = 8.9, 2.5 Hz, 1H), 3.83 (s, 3H), 3.12−3.10 (m, 4H), 3.09 (t, J = 3.4 Hz, 4H), 2.63 (s, 3H); ^{13}C NMR (126 MHz, DMSO-d_6) δ 162.71, 157.45, 139.69, 136.99, 131.83, 125.81, 123.33, 116.59, 106.61, 55.32, 52.87, 45.76, 43.15; MS (ESI) m/z = 291.01 (M + H)$^+$. HRMS (ESI): calcd for ($C_{15}H_{19}N_2O_2S$) 291.11672, found 291.11591 (M + H)$^+$. IR (cm^{-1}): $\tilde{\nu}$ 1620 (C═O).

5-Methoxybenzo[*b*]thiophene-2-carboxylic Acid Benzylamide (2a). The compound was synthesized according to procedure C (with the exception of the reaction time being limited to 2 h), using benzylamine to give a yellow solid: yield 0.015 g (10.7%). The product was purified by CC (DCM/petroleum ether 3:1); mp 208−209 °C; ^{1}H NMR (500 MHz, DMSO-d_6) δ 9.31 (t, J = 6.0 Hz, 1H), 8.04 (s, 1H), 7.89 (d, J = 8.9 Hz, 1H), 7.43 (d, J = 2.5 Hz, 1H), 7.36−7.33 (m, 4H), 7.28−7.25 (m, 1H), 7.10 (dd, J = 8.9, 2.5 Hz, 1H), 4.49 (d, J = 6.0 Hz, 2H), 3.83 (s, 3H); ^{13}C NMR (126 MHz, DMSO-d_6) δ 161.51, 157.37, 140.87, 140.28, 139.28, 132.67, 128.34, 127.30, 126.88, 124.61, 123.57, 116.67, 106.73, 55.39, 42.64; MS (ESI) m/z = 298.03 (M + H)$^+$. HRMS (ESI): calcd for ($C_{17}H_{16}NO_2S$) 298.09017, found 298.08941 (M + H)$^+$. IR (cm^{-1}): $\tilde{\nu}$ 3279 (NH), 1609 (C═O).

(5-Methoxybenzo[*b*]thiophen-2-yl)piperidin-1-ylmethanone(3a). The compound was synthesized according to procedure C, using piperidine to give a white solid: yield 0.04 g (30.8%). The product was purified by CC (DCM/petroleum ether 2:1); mp 90.9 °C; ^{1}H NMR (500 MHz, DMSO-d_6) δ 7.87 (d, J = 8.9 Hz, 1H), 7.57 (s, 1H), 7.44 (d, J = 2.5 Hz, 1H), 7.07 (dd, J = 8.8, 2.5 Hz, 1H), 3.82 (s, 3H), 3.63−3.59 (m, 4H), 1.68−1.63 (m, 2H), 1.59−1.54 (m, 4H); ^{13}C NMR (126 MHz, DMSO-d_6) δ 162.27, 157.37, 139.74, 138.24, 131.44, 124.52, 123.22, 116.15, 106.51, 55.29, 54.87, 23.98; MS (ESI) m/z = 275.97 (M + H)$^+$. HRMS (ESI): calcd for ($C_{15}H_{18}NO_2S$) 276.10582, found 276.10524 (M + H)$^+$. IR (cm^{-1}): $\tilde{\nu}$ 1608 (C═O).

(5-Methoxybenzo[*b*]thiophen-2-yl)morpholin-4-ylmethanone (4a). The compound was synthesized according to procedure C, using morpholine to give a yellow solid: yield 0.05 g (28%). The product was purified by CC (ethyl acetate/hexane 1:1); mp 109−110 °C; ^{1}H NMR (500 MHz, DMSO-d_6) δ 7.88 (d, J = 8.9 Hz, 1H), 7.65 (d, J = 0.6 Hz, 1H), 7.44 (d, J = 2.5 Hz, 1H), 7.09 (dd, J = 8.9, 2.6 Hz, 1H), 3.82 (s, 3H), 3.70−3.67 (m, 4H), 3.66−3.63 (m, 4H); ^{13}C NMR (126 MHz, $CDCl_3$) δ 164.51, 158.39, 140.16, 137.69, 133.23, 125.75, 123.62, 117.14, 106.68, 67.42, 56.08, 26.46, 26.27; MS (ESI) m/z = 278 (M + H)$^+$. HRMS (ESI): calcd for ($C_{14}H_{16}NO_3S$) 278.08509, found 278.08447 (M + H)$^+$. IR (cm^{-1}): $\tilde{\nu}$ 1600 (C═O).

5-Methoxybenzo[*b*]thiophene-2-carboxylic Acid Allylamide (5a). The compound was synthesized according to procedure C, using allylamine to give an orange solid: yield 0.05 g (42%). The product was purified by CC (DCM); mp 130−131 °C; ^{1}H NMR (300 MHz, DMSO-d_6) δ 8.94 (t, J = 5.6 Hz, 1H), 8.02 (s, 1H), 7.89 (d, J = 8.8 Hz, 1H), 7.43 (d, J = 2.5 Hz, 1H), 7.10 (dd, J = 8.8, 2.5 Hz, 1H), 5.92 (ddt, J = 17.1, 10.4, 5.3 Hz, 1H), 5.21 (dd, J = 17.2, 1.7 Hz, 1H), 5.13 (dd, J = 10.2, 1.6 Hz, 1H), 3.92 (t, J = 5.5 Hz, 2H), 3.84 (s, 3H); ^{13}C NMR (75 MHz, DMSO-d_6) δ 161.80, 157.87, 141.44, 140.78, 135.61, 133.13, 124.96, 124.04, 117.13, 115.94, 107.21, 55.89, 42.01; MS (ESI) m/z = 247.99 (M + H)$^+$. HRMS (ESI): calcd for ($C_{13}H_{14}NO_2S$) 248.07452, found 248.07393 (M + H)$^+$. IR (cm^{-1}): $\tilde{\nu}$ 3303 (NH), 1617 (C═O).

5-Methoxybenzo[*b*]thiophene-2-carboxylic Acid Cyclopropylamide (6a). The compound was synthesized according to procedure C, using cyclopropylamine to give an orange solid: yield 0.04 g (33.7%). The product was purified by CC (DCM); mp 164−165 °C; ^{1}H NMR (300 MHz, DMSO-d_6) δ 8.73 (d, J = 3.8 Hz, 1H), 7.94 (s, 1H), 7.88 (d, J = 8.9 Hz, 1H), 7.41 (d, J = 2.5 Hz, 1H), 7.10 (dd, J = 8.9, 2.5 Hz, 1H), 3.83 (s, 3H), 2.85 (ddd, J = 11.1, 7.5, 3.9 Hz, 1H), 0.73 (dt, J = 7.0, 4.9 Hz, 2H), 0.60 (dt, J = 5.7, 4.0 Hz, 2H); ^{13}C

DOI: 10.1021/acs.jmedchem.6b01915
J. Med. Chem. XXXX, XXX, XXX−XXX

NMR (75 MHz, DMSO-d_6) δ 163.17, 157.85, 141.55, 140.77, 133.10, 124.88, 124.04, 117.01, 107.21, 55.89, 23.48, 6.25; MS (ESI) m/z = 248.02 $(M + H)^+$. HRMS (ESI): calcd for ($C_{13}H_{14}NO_2S$) 248.07452, found 248.07391 $(M + H)^+$. IR (cm^{-1}): $\tilde{\nu}$ 3254 (NH), 1621 (C═O).

5-Methoxybenzo[*b*]thiophene-2-carboxylic Acid (2-Hydroxyethyl)amide (7a). The compound was synthesized according to procedure C, using ethanolamine to give a white solid: yield 0.042 g (34.8%). The product was purified by CC (DCM/MeOH 100:3); mp 119−120 °C; ^{1}H NMR (500 MHz, MeOD) δ 7.87 (s, 1H), 7.76 (d, J = 8.9 Hz, 1H), 7.37 (d, J = 2.5 Hz, 1H), 7.09 (dd, J = 8.9, 2.5 Hz, 1H), 3.87 (s, 3H), 3.72 (t, J = 5.8 Hz, 2H), 3.51 (t, J = 5.9 Hz, 2H); ^{13}C NMR (126 MHz, MeOD) δ 165.10, 159.45, 141.84, 141.01, 134.92, 126.33, 124.29, 118.33, 107.40, 61.57, 55.97, 43.58; MS (ESI) m/z = 251.93 $(M + H)^+$. HRMS (ESI): calcd for ($C_{12}H_{14}NO_3S$) 252.06944, found 252.06878 $(M + H)^+$. IR (cm^{-1}): $\tilde{\nu}$ 3537 (OH), 3311 (NH), 1615 (C═O).

[(5-Methoxybenzo[*b*]thiophene-2-carbonyl)amino]acetic Acid Methyl Ester (8a). The compound was synthesized according to procedure C, using glycine methyl ester to give a white solid: yield 0.035 g (26.2%). The product was purified by CC (DCM); mp 121−122 °C; ^{1}H NMR (500 MHz, MeOD) δ 7.90 (s, 1H), 7.78 (d, J = 8.9 Hz, 1H), 7.39 (d, J = 2.4 Hz, 1H), 7.10 (dd, J = 8.9, 2.5 Hz, 1H), 4.13 (s, 2H), 3.87 (s, 3H), 3.76 (s, 3H); ^{13}C NMR (126 MHz, DMSO-d_6) δ 170.18, 162.00, 157.42, 140.20, 139.97, 132.73,125.15, 123.60, 116.92, 106.80, 55.41, 51.83, 41.14 ; MS (ESI) m/z = 279.01 $(M)^+$. HRMS (ESI): calcd for ($C_{13}H_{14}NO_4S$) 280.06435, found 280.06357 $(M + H)^+$. IR (cm^{-1}): $\tilde{\nu}$ 3390 (NH), 1728 (C═O), 1645 (C═O).

[(5-Methoxybenzo[*b*]thiophene-2-carbonyl)amino]acetic Acid (8c). The compound was synthesized according to procedure B, using compound **8a** to give a white solid: yield 0.015 g (95%); mp 121.2 °C; ^{1}H NMR (500 MHz, MeOD) δ 7.90 (d, J = 0.6 Hz, 1H), 7.77 (d, J = 8.9 Hz, 1H), 7.39 (d, J = 2.5 Hz, 1H), 7.10 (dd, J = 8.9, 2.5 Hz, 1H), 4.09 (s, 2H), 3.87 (s, 3H); ^{13}C NMR (126 MHz, MeOD) δ 173.11, 165.31, 159.60, 141.91, 140.47, 135.18, 126.95, 124.46, 118.65, 107.60, 56.13, 42.38; MS (ESI) m/z = 265 $(M)^+$. HRMS (ESI): calcd for ($C_{12}H_{12}NO_4S$) 266.04870, found 266.04776 $(M + H)^+$. IR (cm^{-1}): $\tilde{\nu}$ 3324 (NH), 3000−2980 (OH), 1736 (C═O), 1618 (C═O).

(*S*)-Methyl 2-(5-Methoxybenzo[*b*]thiophene-2-carboxamido)-3-methylbutanoate (9a). The compound was synthesized according to procedure C, using L-valine methyl ester to give a yellow solid: yield 0.14 g (91%). The product was purified by CC (DCM); mp 124.7 °C; ^{1}H NMR (500 MHz, MeOD) δ 8.00 (s, 1H), 7.76 (d, J = 8.9 Hz, 1H), 7.38 (d, J = 2.5 Hz, 1H), 7.10 (dd, J = 8.9, 2.5 Hz, 1H), 4.49 (d, J = 7.0 Hz, 1H), 3.87 (s, 3H), 3.76 (s, 3H), 2.28 (dq, J = 13.7, 6.8 Hz, 1H), 1.06 (d, J = 6.8 Hz, 3H), 1.03 (d, J = 6.8 Hz, 3H); ^{13}C NMR (126 MHz, MeOD) δ 173.63, 165.05, 159.49, 141.82, 140.30, 135.12, 126.93, 124.31, 118.48, 107.57, 60.19, 56.00, 52.55, 31.79, 19.62, 19.15; MS (ESI) m/z = 322.03 $(M + H)^+$. HRMS (ESI): calcd for ($C_{16}H_{20}NO_4S$) 322.11130, found 322.11071 $(M + H)^+$.

(*S*)-2-[(5-Methoxybenzo[*b*]thiophene-2-carbonyl)amino]-3-methylbutyric Acid (9c). The compound was synthesized according to procedure B, using compound **9a** to give a yellow solid: yield 0.08 g (60.2%); mp 137.6 °C; ^{1}H NMR (500 MHz, MeOD) δ 8.00 (s, 1H), 7.97 (s, 1H), 7.75 (d, J = 8.9 Hz, 1H), 7.37 (s, 1H), 7.08 (dd, J = 8.9, 2.5 Hz, 1H), 4.50 (d, J = 6.4 Hz, 1H), 3.86 (s, 3H), 2.30 (dq, J = 13.5, 6.8 Hz, 1H), 1.07 (d, J = 3.9 Hz, 3H), 1.06 (d, J = 3.9 Hz, 3H); ^{13}C NMR (126 MHz, DMSO-d_6) δ 172.88, 161.91, 157.36, 140.32, 140.29, 132.77, 125.40, 123.55, 116.63, 106.85, 58.40, 55.38, 29.53, 19.27, 18.73; MS (ESI) m/z = 308.01 $(M + H)^+$. HRMS (ESI): calcd for ($C_{15}H_{18}NO_4S$) 308.09565, found 308.09483 $(M + H)^+$. IR (cm^{-1}): $\tilde{\nu}$ 3305 (NH), 2960−2930 (OH), 1718 (C═O), 1631(C═O).

(*S*)-2-[(5-Methoxybenzo[*b*]thiophene-2-carbonyl)amino]-propionic Acid Ethyl Ester (10a). The compound was synthesized according to procedure C, using L-alanine ethyl ester to give a yellowish white solid: yield 0.09 g (57%). The product was purified by CC (DCM); mp 101.5 °C; ^{1}H NMR (500 MHz, MeOD) δ 7.95 (s, 1H), 7.76 (d, J = 8.9 Hz, 1H), 7.37 (d, J = 2.5 Hz, 1H), 7.09 (dd, J = 8.9, 2.5 Hz, 1H), 4.60 (q, J = 7.3 Hz, 1H), 4.22 (q, J = 7.1 Hz, 2H), 3.86 (s, 3H), 1.53 (d, J = 7.3 Hz, 3H), 1.29 (t, J = 7.1 Hz, 3H); ^{13}C NMR (126 MHz, MeOD) δ 174.24, 164.72, 159.44, 141.81, 140.39, 135.07, 126.84, 124.31, 118.48, 107.45, 62.45, 55.98, 50.28, 17.26, 14.48; MS (ESI) m/z = 307.95 $(M + H)^+$. HRMS (ESI): calcd for ($C_{15}H_{18}NO_4S$) 308.09565, found 308.09479 $(M + H)^+$. IR (cm^{-1}): $\tilde{\nu}$ 3400 (NH), 1731 (C═O), 1646 (C═O).

(*S*)-2-[(5-Methoxybenzo[*b*]thiophene-2-carbonyl)amino]-propionic Acid (10c). The compound was synthesized according to procedure B, using compound **10a** to give a white solid: yield 0.043 g (95.6%); mp 187.8 °C. ^{1}H NMR (500 MHz, MeOD) δ 7.95 (d, J = 0.5 Hz, 1H), 7.76 (d, J = 8.9 Hz, 1H), 7.37 (d, J = 2.5 Hz, 1H), 7.09 (dd, J = 8.9, 2.5 Hz, 1H), 4.60 (q, J = 7.3 Hz, 1H), 3.87 (s, 3H), 1.54 (d, J = 7.4 Hz, 3H); ^{13}C NMR (126 MHz, MeOD) δ 176.32, 164.97, 159.78, 142.17, 140.88, 135.39, 127.10, 124.63, 118.77, 107.78, 56.31, 50.31, 17.84; MS (ESI) m/z = 279.88 $(M + H)^+$. HRMS (ESI): calcd for ($C_{13}H_{14}NO_4S$) 280.06435, found 280.06352 $(M + H)^+$. IR (cm^{-1}): $\tilde{\nu}$ 3324 (NH), 2960−2930 (OH), 1708 (C═O), 1622 (C═O).

5-Methoxybenzo[*b*]thiophene-2-carboxylic Acid (2-Aminoethyl)amide (11a). The compound was synthesized according to procedure C, using ethylenediamine to give an orange solid: yield 0.06 g (38.4%). The product was purified by CC (DCM/MeOH/TEA 100:2:1); mp 100.2 °C; ^{1}H NMR (500 MHz, MeOD) δ 7.87 (s, 1H), 7.75 (d, J = 8.9 Hz, 1H), 7.36 (d, J = 2.4 Hz, 1H), 7.08 (dd, J = 8.9, 2.5 Hz, 1H), 3.85 (s, 3H), 3.74−3.72 (m, 2H), 3.47 (t, J = 6.4 Hz, 2H), 3.02 (s, 1H), 2.98 (s, 2H); ^{13}C NMR (126 MHz, MeOD) δ 165.19, 159.43, 141.84, 140.96, 134.91, 126.39, 124.31, 118.36, 107.44, 56.01, 43.41, 41.99; MS (ESI) m/z = 250.94 $(M + H)^+$. HRMS (ESI): calcd for ($C_{12}H_{15}N_2O_2S$) 251.08542, found 251.08457 $(M + H)^+$. IR (cm^{-1}): $\tilde{\nu}$ 3260−3200 (NH_2), 3065 (NH), 1620 (C═O).

5-Methoxybenzo[*b*]thiophene-2-carboxylic Acid Phenylamide (12a). The compound was synthesized according to procedure C, using aniline to give a yellow solid: yield 0.03 g (25%). The product was purified by CC (DCM/petroleum ether 3:1); mp 169.8 °C; ^{1}H NMR (500 MHz, MeOD) δ 8.08 (d, J = 0.5 Hz, 1H), 7.80 (d, J = 8.9 Hz, 1H), 7.71−7.70 (m, 1H), 7.70−7.68 (m, 1H), 7.42 (d, J = 2.5 Hz, 1H), 7.40−7.36 (m, 2H), 7.19−7.15 (m, 1H), 7.12 (dd, J = 8.9, 2.5 Hz, 1H), 3.89 (s, 3H); ^{13}C NMR (126 MHz, MeOD) δ 163.17, 159.50, 141.91, 141.68, 139.50, 135.27, 129.88, 126.77, 125.76, 124.34, 122.26, 118.56, 107.53, 56.00; MS (ESI) m/z = 283.95 $(M + H)^+$. HRMS (ESI): calcd for ($C_{16}H_{14}NO_2S$) 284.07452, found 284.07371 $(M + H)^+$.

(*R*)-5-Methoxybenzo[*b*]thiophene-2-carboxylic Acid (1,2,2-Trimethylpropyl)amide (13a). The compound was synthesized according to procedure C, using (*R*)-3,3-dimethyl-2-butylamine to give a white solid: yield 0.1 g (71.4%). The product was purified by CC (DCM); mp 155.3 °C; ^{1}H NMR (500 MHz, DMSO-d_6) δ 8.19 (d, J = 9.4 Hz, 1H), 8.09 (s, 1H), 7.86 (d, J = 8.8 Hz, 1H), 7.41 (d, J = 2.5 Hz, 1H), 7.09 (dd, J = 8.8, 2.5 Hz, 1H), 3.94 (dq, J = 13.9, 6.9 Hz, 1H), 3.82 (s, 3H), 1.11 (d, J = 6.9 Hz, 3H), 0.91 (s, 9H); ^{13}C NMR (126 MHz, $CDCl_3$) δ 161.06, 157.32, 141.48, 140.31, 132.63, 124.35, 123.54, 116.27, 106.83, 55.38, 52.63, 34.76, 26.36, 15.47; MS (ESI) m/z = 291.99 $(M + H)^+$. HRMS (ESI): calcd for ($C_{16}H_{22}NO_2S$) 292.13712, found 292.13625 $(M + H)^+$. IR (cm^{-1}): $\tilde{\nu}$ 3310 (NH), 1616 (C═O).

5-Methoxybenzo[*b*]thiophene-2-carboxylic Acid (2,2,2-Trifluoroethyl)amide (14a). The compound was synthesized according to procedure C, using 2,2,2-trifluoroethylamine to give a yellow solid: yield 0.02 g (14.8%). The product was purified by CC (DCM/petroleum ether 2:1); mp 130.8 °C; ^{1}H NMR (500 MHz, MeOD) δ 7.92 (s, 1H), 7.77 (d, J = 8.9 Hz, 1H), 7.38 (d, J = 2.5 Hz, 1H), 7.10 (dd, J = 8.9, 2.5 Hz, 1H), 4.09 (q, J = 9.3 Hz, 2H), 3.86 (s, 3H); ^{13}C NMR (126 MHz, MeOD) δ 163.57, 157.99, 140.18, 138.27, 133.68, 125.64, 124.40 (d, $^1J_{C-F}$ = 278.4 Hz), 122.82, 117.24, 106.00, 54.47, 41.89; MS (ESI) m/z = 289.05 $(M)^+$. HRMS (ESI): calcd for ($C_{12}H_{11}F_3NO_2S$) 290.04626, found 290.04572 $(M + H)^+$. IR (cm^{-1}): $\tilde{\nu}$ 3283 (NH), 1619 (C═O).

5-Methoxybenzo[*b*]thiophene-2-carboxylic Acid Thiazol-2-ylamide (15a). The compound was synthesized according to procedure C, using 2-aminothiazole to give a yellow solid: yield 0.023 g (16.5%). The product was purified by CC (DCM/MeOH 100:1); mp 177.4 °C; ^{1}H NMR (500 MHz, acetone-d_6) δ 8.39 (s, 1H), 7.92 (d, J = 8.9 Hz, 1H), 7.50 (d, J = 3.6 Hz, 1H), 7.48 (d, J = 2.5 Hz,

DOI: 10.1021/acs.jmedchem.6b01915
J. Med. Chem. XXXX, XXX, XXX−XXX

1H), 7.20 (d, J = 3.6 Hz, 1H), 7.17 (dd, J = 8.9, 2.5 Hz, 1H), 3.89 (s, 3H); ^{13}C NMR (126 MHz, acetone-d_6) δ 161.27, 159.30, 159.09, 141.49, 139.44, 138.18, 135.13, 127.69, 124.36, 118.79, 114.51, 107.61, 55.89; MS (ESI) m/z = 290 $(M)^+$. HRMS (ESI): calcd for ($C_{13}H_{11}N_2O_2S_2$) 291.02619, found 291.02539 $(M + H)^+$. IR (cm^{-1}): $\tilde{\nu}$ 3159 (NH), 1670 (C═O).

5-Methoxybenzo[*b*]thiophene-2-carboxylic Acid Benzylmethylamide (16a). The compound was synthesized according to procedure C, using *N*-benzylmethylamine to give a white solid: yield 0.103 g (68.9%). The product was purified by CC (DCM); mp 121.9 °C; ^{1}H NMR (500 MHz, $CDCl_3$) δ 7.69 (d, J = 8.8 Hz, 1H), 7.45−7.37 (m, 3H), 7.36−7.28 (m, 3H), 7.19 (s, 1H), 7.04 (dd, J = 8.7, 1.7 Hz, 1H), 4.81 (s, 2H), 3.84 (s, 3H), 3.13 (s, 3H); ^{13}C NMR (126 MHz, $CDCl_3$) δ 165.22, 157.70, 139.72, 138.34, 136.54, 132.86, 128.87, 127.65, 126.74, 124.87, 123.00, 116.57, 106.08, 55.49, 36.96, 34.36; MS (ESI) m/z = 313.01 $(M + H)^+$. HRMS (ESI): calcd for ($C_{18}H_{18}NO_2S$) 312.10582, found 312.10479 $(M + H)^+$. IR (cm^{-1}): $\tilde{\nu}$ 1613 (C═O).

5-Methoxybenzo[*b*]thiophene-2-carboxylic Acid Phenethylamide (17a). The compound was synthesized according to procedure C, using 2-phenylethylamine to give a white solid: yield 0.11 g (81.7%). The product was purified by CC (DCM/petroleum ether 4:1); mp 153.8 °C; ^{1}H NMR (500 MHz, $CDCl_3$) δ 7.69 (d, J = 8.9 Hz, 1H), 7.61 (s, 1H), 7.36−7.33 (m, 2H), 7.28−7.26 (m, 1H), 7.26−7.24 (m, 2H), 7.22 (d, J = 2.5 Hz, 1H), 7.07 (dd, J = 8.9, 2.5 Hz, 1H), 3.86 (s, 3H), 3.73 (dd, J = 12.9, 6.9 Hz, 2H), 2.95 (t, J = 6.9 Hz, 2H); ^{13}C NMR (126 MHz, DMSO-d_6) δ 161.41, 157.36, 141.14, 140.27, 139.35, 132.58, 128.66, 128.35, 126.13, 124.27, 123.55, 116.58, 106.69, 55.39, 40.91, 35.03; MS (ESI) m/z = 312 $(M + H)^+$. HRMS (ESI): calcd for ($C_{18}H_{18}NO_2S$) 312.10582, found 312.10484 $(M + H)^+$. IR (cm^{-1}): $\tilde{\nu}$ 3337 (NH), 1629 (C═O).

5-Methoxybenzo[*b*]thiophene-2-carboxylic Acid Methylphenethylamide (17b). The compound was synthesized according to procedure D, using compound **17a**, to give a yellow solid: yield 0.012 g (57%). The product was purified by CC (DCM/petroleum ether 4:1); mp 180−181 °C; ^{1}H NMR (500 MHz, DMSO-d_6) δ 7.87 (dd, J = 8.8, 5.5 Hz, 1H), 7.43 (d, J = 2.5 Hz, 1H), 7.32−7.27 (m, 3H), 7.24 (ddd, J = 15.9, 9.2, 4.4 Hz, 3H), 7.08 (ddd, J = 8.4, 5.8, 2.5 Hz, 1H), 3.82 (s, 3H), 3.70 (t, J = 7.2 Hz, 2H), 3.17 (s, 3H), 2.91 (t, J = 6.9 Hz, 2H); ^{13}C NMR (126 MHz, DMSO-d_6) δ 161.45, 157.37, 141.15, 140.30, 139.38, 132.60, 128.78, 128.45, 126.34, 124.30, 123.22, 116.61, 106.59, 55.42, 55.34, 40.94, 35.06; MS (ESI) m/z = 326 $(M + H)^+$. HRMS (ESI): calcd for ($C_{19}H_{20}NO_2S$) 326.12147, found 326.12052 $(M + H)^+$.

5-Methoxybenzo[*b*]thiophene-2-carboxylic Acid (Pyridin-2-ylmethyl)amide (18a). The compound was synthesized according to procedure C, using 2-picolylamine to give a white solid: yield 0.064 (55.85%). The product was purified by CC (DCM/MeOH 100:1); mp 137−138 °C; ^{1}H NMR (500 MHz, MeOD) δ 8.50 (ddd, J = 5.0, 1.8, 0.9 Hz, 1H), 7.94 (d, J = 0.5 Hz, 1H), 7.82 (td, J = 7.8, 1.8 Hz, 1H), 7.77 (d, J = 8.9 Hz, 1H), 7.46 (dt, J = 7.9, 1.0 Hz, 1H), 7.38 (d, J = 2.4 Hz, 1H), 7.34−7.31 (m, 1H), 7.10 (dd, J = 8.9, 2.5 Hz, 1H), 4.70 (s, 2H), 3.86 (s, 3H); ^{13}C NMR (126 MHz, MeOD) δ 165.01, 159.49, 159.24, 149.82, 141.83, 140.63, 138.94, 135.03, 126.70, 124.34, 123.87, 122.95, 118.50, 107.45, 55.98, 45.94; MS (ESI) m/z = 299.01 $(M + H)^+$. HRMS (ESI): calcd for ($C_{16}H_{15}N_2O_2S$) 299.08542, found 299.08468 $(M + H)^+$. IR (cm^{-1}): $\tilde{\nu}$ 3281 (NH), 1610 (C═O).

5-Methoxybenzo[*b*]thiophene-2-carboxylic Acid Methylpyridin-2-ylmethylamide (18b). The compound was synthesized according to procedure D, using compound **18a**, to give a yellow solid: yield 0.025 g (47%). The product was purified by CC (DCM/MeOH 100:2); mp 144.9 °C; ^{1}H NMR (500 MHz, acetone-d_6) δ 8.56 (s, 1H), 7.79 (d, J = 9.2 Hz, 2H), 7.71−7.63 (m, 1H), 7.38−7.35 (m, 2H), 7.28 (s, 1H), 7.04 (d, J = 9.4 Hz, 1H), 4.86 (s, 2H), 3.81 (s, 3H), 3.27 (s, 3H); ^{13}C NMR (126 MHz, acetone-d_6) δ 164.64, 158.87, 150.45, 141.15, 140.18, 137.71, 133.42, 126.11, 123.83, 123.33, 122.56, 117.40, 114.67, 107.20, 56.05, 55.80, 49.80; MS (ESI) m/z = 313 $(M + H)^+$. HRMS (ESI): calcd for ($C_{17}H_{17}N_2O_2S$) 313.10107, found 313.10015 $(M + H)^+$. IR (cm^{-1}): $\tilde{\nu}$ 1604 (C═O).

5-Methoxybenzo[*b*]thiophene-2-carboxylic Acid (Pyridin-3-ylmethyl)amide (19a). The compound was synthesized according to procedure C, using 3-picolylamine to give a white solid: yield 0.051 g (44.5%). The product was purified by CC (DCM/MeOH 100:2); mp 167.3 °C; ^{1}H NMR (500 MHz, MeOD) δ 8.47 (d, J = 1.7 Hz, 1H), 8.35 (dd, J = 4.9, 1.5 Hz, 1H), 7.79−7.76 (m, 2H), 7.65 (d, J = 8.9 Hz, 1H), 7.33 (ddd, J = 7.9, 4.9, 0.8 Hz, 1H), 7.26 (d, J = 2.5 Hz, 1H), 6.98 (dd, J = 8.9, 2.5 Hz, 1H), 4.51 (s, 2H), 3.75 (s, 3H); ^{13}C NMR (126 MHz, MeOD) δ 164.92, 159.49, 149.48, 148.87, 141.79, 140.52, 137.80, 136.75, 135.00, 126.63, 125.33, 124.33, 118.51, 107.45, 55.98, 42.07; MS (ESI) m/z = 298.98 $(M + H)^+$. HRMS (ESI): calcd for ($C_{16}H_{15}N_2O_2S$) 299.08542, found 299.08473 $(M + H)^+$. IR (cm^{-1}): $\tilde{\nu}$ 3276 (NH), 1610 (C═O).

5-Methoxybenzo[*b*]thiophene-2-carboxylic Acid Methylpyridin-3-ylmethylamide (19b). The compound was synthesized according to procedure D, using compound **19a** to give a yellow solid: yield 0.02 g (47.77%). The compound was purified by salting out, through addition of 3 mL of DCM, then addition of 30 mL of petroleum ether to salt out compound **19a** leaving the product in filtrate, which was then filtered over anhydrous $MgSO_4$. The solvent was then removed under reduced pressure to give the final product; mp 132−133 °C; ^{1}H NMR (500 MHz, acetone-d_6) δ 8.62 (s, 1H), 8.54 (dd, J = 4.7, 1.6 Hz, 1H), 7.84 (d, J = 8.9 Hz, 1H), 7.80 (d, J = 7.3 Hz, 1H), 7.69 (s, 1H), 7.41 (dd, J = 7.4, 4.9 Hz, 2H), 7.09 (dd, J = 8.9, 2.5 Hz, 1H), 4.86 (s, 2H), 3.85 (s, 3H), 3.25 (s, 3H); ^{13}C NMR (126 MHz, MeOD) δ 159.56, 149.45, 149.42, 141.40, 137.85, 134.84, 134.81, 125.60, 125.56, 125.39, 124.06, 124.01, 118.20, 107.43, 55.97, 49.85, 30.77; MS (ESI) m/z = 313.03 $(M + H)^+$. HRMS (ESI): calcd for ($C_{17}H_{17}N_2O_2S$) 313.10107, found 313.10021 $(M + H)^+$. IR (cm^{-1}): $\tilde{\nu}$ 1609 (C═O).

5-Methoxybenzo[*b*]thiophene-2-carboxylic Acid 2-Fluorobenzylamide (20a). The compound was synthesized according to procedure C, using 2-fluorobenzylamine to give a white solid: yield 0.134 g (74%). The product was purified by CC (DCM); mp 152.8 °C; ^{1}H NMR (500 MHz, DMSO-d_6) δ 9.30 (t, J = 5.8 Hz, 1H), 8.06 (s, 1H), 7.89 (d, J = 8.9 Hz, 1H), 7.43 (d, J = 2.5 Hz, 1H), 7.41 (td, J = 7.7, 1.6 Hz, 1H), 7.33 (ddd, J = 9.6, 6.4, 1.8 Hz, 1H), 7.22−7.20 (m, 1H), 7.19−7.17 (m, 1H), 7.10 (dd, J = 8.9, 2.5 Hz, 1H), 4.53 (d, J = 5.8 Hz, 2H), 3.83 (s, 3H); ^{13}C NMR (126 MHz, DMSO-d_6) δ 161.62, 160.04 (d, $^1J_{C-F}$ = 244.5 Hz), 157.37, 140.58, 140.25, 132.69, 129.63 (d, $^3J_{C-F}$ = 4.4 Hz), 129.01 (d, $^3J_{C-F}$ = 8.1 Hz), 125.76 (d, $^2J_{C-F}$ = 14.7 Hz), 124.81 (s), 124.36 (d, $^4J_{C-F}$ = 3.4 Hz), 123.56, 116.71, 115.12 (d, $^2J_{C-F}$ = 21.1 Hz), 106.74, 55.38, 36.51 (d, $^3J_{C-F}$ = 4.6 Hz); MS (ESI) m/z = 315.98 $(M + H)^+$. HRMS (ESI): calcd for ($C_{17}H_{15}FNO_2S$) 316.08075, found 316.08001 $(M + H)^+$. IR (cm^{-1}): $\tilde{\nu}$ 3288 (NH), 1612 (C═O).

5-Methoxybenzo[*b*]thiophene-2-carboxylic Acid (2-Fluorobenzyl)methylamide (20b). The compound was synthesized according to procedure D using compound **20a**, to give a yellowish white solid: yield 0.065 g (62.5%). The product was purified by CC (DCM); mp 110−111 °C; ^{1}H NMR (500 MHz, DMSO-d_6) δ 7.88 (d, J = 8.9 Hz, 1H), 7.78 (s, 1H), 7.43 (s, 1H), 7.38 (ddd, J = 12.7, 8.9, 4.3 Hz, 2H), 7.24 (t, J = 9.0 Hz, 2H), 7.11−7.07 (m, 1H), 4.80 (s, 2H), 3.81 (s, 3H), 3.22 (s, 3H); ^{13}C NMR (126 MHz, DMSO-d_6) δ 160.37 (d, $^1J_{C-F}$ = 245.9 Hz), 157.37, 140.59, 139.90, 138.40, 131.85, 129.52 (d, $^3J_{C-F}$ = 4.6 Hz), 129.47, 124.72, 123.73 (d, $^2J_{C-F}$ = 14.4 Hz), 123.57, 123.23, 116.58, 115.46 (d, $^2J_{C-F}$ = 20.9 Hz), 106.63, 55.39, 55.30, 45.92; MS (ESI) m/z = 329.99 $(M + H)^+$. HRMS (ESI): calcd for ($C_{18}H_{17}FNO_2S$) 330.09640, found 330.09567 $(M + H)^+$. IR (cm^{-1}): $\tilde{\nu}$ 1601 (C═O).

5-Methoxybenzo[*b*]thiophene-2-carboxylic Acid 3-Fluorobenzylamide (21a). The compound was synthesized according to procedure C, using 3-fluorobenzylamine to give a white solid: yield 0.13 g (71.5%). The product was purified by CC (DCM); mp 164.9 °C; ^{1}H NMR (500 MHz, DMSO-d_6) δ 9.35 (t, J = 6.0 Hz, 1H), 8.05 (d, J = 0.6 Hz, 1H), 7.91−7.88 (m, 1H), 7.44 (d, J = 2.4 Hz, 1H), 7.39 (ddd, J = 10.7, 7.0, 5.1 Hz, 1H), 7.20−7.17 (m, 1H), 7.17−7.13 (m, 1H), 7.12−7.07 (m, 2H), 4.50 (d, J = 6.0 Hz, 2H), 3.83 (s, 3H); ^{13}C NMR (126 MHz, DMSO-d_6) δ 162.20 (d, $^1J_{C-F}$ = 243.4 Hz), 161.28, 157.38, 142.29 (d, $^3J_{C-F}$ = 7.0 Hz), 140.59, 140.25,

DOI: 10.1021/acs.jmedchem.6b01915
J. Med. Chem. XXXX, XXX, XXX−XXX

132.69, 130.31 (d, $^3J_{C-F}$ = 8.3 Hz), 124.78, 123.57, 123.25 (d, $^4J_{C-F}$ = 2.6 Hz), 116.73, 113.93 (d, $^2J_{C-F}$ = 21.5 Hz), 113.64 (d, $^2J_{C-F}$ = 20.9 Hz), 106.74, 55.38, 42.17 (d, $^4J_{C-F}$ = 1.2 Hz); MS (ESI) m/z = 315.98 $(M + H)^+$. HRMS (ESI): calcd for ($C_{17}H_{15}FNO_2S$) 316.08075, found 316.08003 $(M + H)^+$. IR (cm^{-1}): $\tilde{\nu}$ 3286 (NH), 1614 (C═O).

5-Methoxybenzo[*b*]thiophene-2-carboxylic Acid (3-Fluorobenzyl)methylamide (21b). The compound was synthesized according to procedure D, using compound **21a** to give a white solid: yield 0.05 g (48%). The product was purified by CC (DCM); mp 109.6 °C; ^{1}H NMR (500 MHz, DMSO-d_6) δ 7.89 (dd, J = 8.8, 4.3 Hz, 1H), 7.47−7.41 (m, 2H), 7.20−7.06 (m, 5H), 4.76 (s, 2H), 3.80 (s, 3H), 3.22 (s, 3H); ^{13}C NMR (126 MHz, DMSO-d_6) δ 162.39 (d, $^1J_{C-F}$ = 243.1 Hz), 161.64, 157.37, 140.13 (d, $^3J_{C-F}$ = 6.5 Hz), 139.93, 138.44, 132.71 131.85, 130.69 (d, $^3J_{C-F}$ = 8.0 Hz), 124.79, 123.58, 116.60, 114.15 (d, $^2J_{C-F}$ = 20.7 Hz), 113.65 (d, $^2J_{C-F}$ = 21.2 Hz), 106.63, 55.30, 42.19, 37.29; MS (ESI) m/z = 330.01 $(M + H)^+$. HRMS (ESI): calcd for ($C_{18}H_{17}FNO_2S$) 330.09640, found 330.09556 $(M + H)^+$. IR (cm^{-1}): $\tilde{\nu}$ 1612 (C═O).

5-Methoxybenzo[*b*]thiophene-2-carboxylic Acid 4-Fluorobenzylamide (22a). The compound was synthesized according to procedure C, using 4-fluorobenzylamine to give a white solid: yield 0.11 g (73%). The product was purified by CC (DCM); mp 185.8 °C; ^{1}H NMR (500 MHz, DMSO-d_6) δ 9.31 (d, J = 4.9 Hz, 1H), 8.02 (d, J = 3.8 Hz, 1H), 7.88 (dd, J = 8.8, 3.9 Hz, 1H), 7.43 (d, J = 2.7 Hz, 1H), 7.41−7.35 (m, 2H), 7.20−7.14 (m, 2H), 7.12−7.08 (m, 1H), 4.47 (d, J = 3.9 Hz, 2H), 3.83 (s, 3H); ^{13}C NMR (126 MHz, DMSO-d_6) δ 161.51, 161.20 (d, $^1J_{C-F}$ = 241.5 Hz), 157.36, 140.75, 140.25, 135.46 (d, $^4J_{C-F}$ = 2.7 Hz), 132.67, 129.31 ($^3J_{C-F}$, J = 8.1 Hz), 124.66, 123.56, 116.68, 115.05 (d, $^2J_{C-F}$ = 21.3 Hz), 106.72, 55.37, 41.96; MS (ESI) m/z = 316 $(M + H)^+$. HRMS (ESI): calcd for ($C_{17}H_{15}FNO_2S$) 316.08075, found 316.08010 $(M + H)^+$. IR (cm^{-1}): $\tilde{\nu}$ 3279 (NH), 1615 (C═O).

5-Methoxybenzo[*b*]thiophene-2-carboxylic Acid (4-Fluorobenzyl)methylamide (22b). The compound was synthesized according to procedure D, using compound **22a** to give a yellow solid: yield 0.05 g (53.19%). The compound was purified by salting out, through addition of 3 mL DCM, followed by the addition of 30 mL of petroleum ether that will salt out compound **22a** leaving the product in the filtrate, which was then filtered over anhydrous $MgSO_4$. The solvent was then removed under reduced pressure to give the final product; mp 125−126 °C; ^{1}H NMR (500 MHz, acetone-d_6) δ 7.85−7.81 (m, 1H), 7.64 (d, J = 8.8 Hz, 1H), 7.45−7.37 (m, 3H), 7.16 (t, J = 8.7 Hz, 2H), 7.08 (dd, J = 8.9, 2.5 Hz, 1H), 4.80 (s, 2H), 3.84 (s, 3H), 3.18 (s, 3H); ^{13}C NMR (126 MHz, DMSO-d_6) δ 161.47 (d, $^1J_{C-F}$ = 242.9 Hz), 157.37, 140.77, 140.27, 139.92, 131.82, 129.32 (d, $^3J_{C-F}$ = 8.1 Hz), 124.68, 123.56, 123.22, 116.56, 115.47 (d, $^2J_{C-F}$ = 21.1 Hz), 106.62, 55.38, 55.30, 41.97; MS (ESI) m/z = 330 $(M + H)^+$. HRMS (ESI): calcd for ($C_{18}H_{17}FNO_2S$) 330.09640, found 330.09566 $(M + H)^+$. IR (cm^{-1}): $\tilde{\nu}$ 1601 (C═O).

5-Methoxybenzo[*b*]thiophene-2-carboxylic Acid 3-Methoxybenzylamide (23a). The compound was synthesized according to procedure C, using 3-methoxybenzylamine, to give a white solid: yield 0.12 g (63.6%). The product was purified by CC (DCM); mp 147.1 °C; ^{1}H NMR (500 MHz, DMSO-d_6) δ 9.29 (t, J = 6.0 Hz, 1H), 8.04 (d, J = 0.6 Hz, 1H), 7.89 (dd, J = 8.9, 0.6 Hz, 1H), 7.43 (d, J = 2.4 Hz, 1H), 7.28−7.24 (m, 1H), 7.10 (dd, J = 8.9, 2.5 Hz, 1H), 6.92−6.90 (m, 2H), 6.84−6.82 (m, 1H), 4.46 (d, J = 6.0 Hz, 2H), 3.83 (s, 3H), 3.74 (s, 3H); ^{13}C NMR (126 MHz, DMSO-d_6) δ 161.50, 159.30, 157.36, 140.86, 140.84, 140.27, 132.67, 129.42, 124.61, 123.56, 119.42, 116.67, 113.02, 112.17, 106.72, 55.37, 54.96, 42.58; MS (ESI) m/z = 328.02 $(M + H)^+$. HRMS (ESI): calcd for ($C_{18}H_{18}NO_3S$) 328.10074, found 328.09998 $(M + H)^+$. IR (cm^{-1}): $\tilde{\nu}$ 3290 (NH), 1610 (C═O).

5-Methoxybenzo[*b*]thiophene-2-carboxylic Acid (3-Methoxybenzyl)methylamide (23b). The compound was synthesized according to procedure D, using compound **23a** to give a yellow solid: yield 0.05 g (42%). The compound was purified by salting out, through addition of a 3 mL of DCM, then addition of 30 mL of petroleum ether to salt out compound **23a** leaving the product in the filtrate. which was then filtered over $MgSO_4$. Then the solvent was removed under reduced pressure to give the final product; mp 111.7 °C; ^{1}H NMR (500 MHz, DMSO-d_6) δ 7.88 (d, J = 8.8 Hz, 1H), 7.42 (s, 1H), 7.31 (t, J = 7.9 Hz, 1H), 7.11−7.06 (m, 1H), 6.95−6.76 (m, 4H), 4.72 (s, 2H), 3.80 (s, 3H), 3.75 (s, 3H), 3.19 (s, 3H); ^{13}C NMR (126 MHz, DMSO-d_6) δ 161.52, 159.54, 157.37, 140.87, 139.91, 138.63, 131.79, 129.84, 124.63, 123.56, 123.22, 119.44, 116.54, 112.64, 106.61, 55.39, 55.30, 54.99, 42.59 ; MS (ESI) m/z = 342.02 $(M + H)^+$. HRMS (ESI): calcd for ($C_{19}H_{20}NO_3S$) 342.11639, found 342.11554$(M + H)^+$. IR (cm^{-1}): $\tilde{\nu}$ 1617 (C═O).

5-Methoxybenzo[*b*]thiophene-2-carboxylic Acid Methyl-(3-methylbenzyl)amide (24a). The compound was synthesized according to procedure C, using *N*-methyl-1-(*m*-tolyl)methanamine to give a yellow solid: yield 0.134 g (73.6%). The product was purified by CC (DCM); mp 125.7 °C; ^{1}H NMR (500 MHz, DMSO-d_6) δ 7.88 (d, J = 8.8 Hz, 1H), 7.79 (s, 1H), 7.42 (s, 1H), 7.28 (t, J = 7.5 Hz, 1H), 7.10 (dd, J = 16.0, 7.9 Hz, 4H), 4.71 (s, 2H), 3.80 (s, 3H), 3.17 (s, 3H), 2.31 (s, 3H); ^{13}C NMR (126 MHz, DMSO-d_6) δ 163.37, 157.36, 139.90, 138.53, 137.86, 136.90, 131.78, 128.61, 128.00, 126.09, 124.60, 123.87, 123.21, 116.51, 106.60, 55.29, 51.07, 37.19, 21.02; MS (ESI) m/z = 325.95 $(M + H)^+$. HRMS (ESI): calcd for ($C_{19}H_{20}NO_2S$) 326.12147, found 342.12078$(M + H)^+$. IR (cm^{-1}): $\tilde{\nu}$ 1614 (C═O).

5-Methoxybenzo[*b*]thiophene-2-carboxylic Acid (Furan-2-ylmethyl)amide (25a). The compound was synthesized according to procedure C, using furfurylamine to give a yellow solid: yield 0.1 g (58%). The product was purified by CC (DCM); mp 118.9 °C; ^{1}H NMR (500 MHz, DMSO-d_6) δ 9.24 (t, J = 5.6 Hz, 1H), 8.03 (s, 1H), 7.88 (d, J = 8.9 Hz, 1H), 7.60 (dd, J = 1.8, 0.9 Hz, 1H), 7.42 (d, J = 2.5 Hz, 1H), 7.10 (dd, J = 8.9, 2.5 Hz, 1H), 6.41 (dd, J = 3.2, 1.8 Hz, 1H), 6.31 (dd, J = 3.2, 0.7 Hz, 1H), 4.47 (d, J = 5.7 Hz, 2H), 3.82 (s, 3H); ^{13}C NMR (126 MHz, DMSO-d_6) δ 161.38, 157.36, 151.94, 142.16, 140.58, 140.24, 132.68, 124.79, 123.55, 116.73, 110.50, 107.16, 106.71, 55.37, 35.97; MS (ESI) m/z = 288 $(M + H)^+$. HRMS (ESI): calcd for ($C_{15}H_{14}NO_3S$) 288.06944, found 288.06872$(M + H)^+$. IR (cm^{-1}): $\tilde{\nu}$ 3306 (NH), 1616 (C═O).

5-Methoxybenzo[*b*]thiophene-2-carboxylic Acid (2-Imidazol-1-ylethyl)amide (26a). The compound was synthesized according to procedure C, using 2-(1*H*-imidazol-1-yl)ethanamine to give a white solid: yield 0.025 g (34.7%). The product was purified by CC (DCM/MeOH 100:3); mp 143 °C; ^{1}H NMR (500 MHz, MeOD) δ 7.88 (s, 1H), 7.78 (d, J = 0.5 Hz, 1H), 7.74 (d, J = 8.9 Hz, 1H), 7.34 (d, J = 2.4 Hz, 1H), 7.24 (s, 1H), 7.08 (dd, J = 8.9, 2.5 Hz, 2H), 4.33−4.29 (m, 2H), 3.85 (s, 3H), 3.75−3.72 (m, 2H); ^{13}C NMR (126 MHz, MeOD) δ 165.15, 159.49, 141.74, 140.38, 138.39, 134.94, 127.83, 126.60, 124.31, 121.49, 118.53, 107.44, 55.99, 47.56, 41.77; MS (ESI) m/z = 302 $(M + H)^+$. HRMS (ESI): calcd for ($C_{15}H_{16}N_3O_2S$) 302.09632, found 302.09546 $(M + H)^+$. IR (cm^{-1}): $\tilde{\nu}$ 3300 (NH), 1612 (C═O).

5-Methoxybenzo[*b*]thiophene-2-carboxylic Acid (2-Imidazol-1-yl-ethyl)methylamide (26b). The compound was synthesized according to procedure D, using compound **26a** to give a white solid: yield 0.08 g (36%). The product was purified by CC (DCM/MeOH 100:2.5); mp 117−118 °C; ^{1}H NMR (500 MHz, acetone-d_6) δ 7.82 (d, J = 8.8 Hz, 1H), 7.63 (s, 1H), 7.51 (d, J = 2.4 Hz, 1H), 7.40 (s, 1H), 7.16 (dd, J = 8.9, 2.5 Hz, 1H), 7.08 (dd, J = 8.8, 2.5 Hz, 1H), 6.97 (s, 1H), 4.37 (t, J = 6.0 Hz, 2H), 3.91 (t, J = 5.9 Hz, 2H), 3.86 (s, 3H), 3.10 (s, 3H); ^{13}C NMR (126 MHz, DMSO-d_6) δ 157.34, 139.88, 139.84, 137.42, 131.73, 128.18, 128.16, 123.20, 119.76, 119.72, 116.45, 106.58, 55.31, 54.89, 43.66, 29.00; MS (ESI) m/z = 315.97 $(M + H)^+$. HRMS (ESI): calcd for ($C_{16}H_{18}N_3O_2S$) 316.11197, found 316.11123 $(M + H)^+$. IR (cm^{-1}): $\tilde{\nu}$ 1626 (C═O).

5-Methoxybenzo[*b*]thiophene-2-carboxylic Acid (1*H*-Imidazol-2-ylmethyl)amide (27a). The compound was synthesized according to procedure C, using 2-aminomethyl-1*H*-imidazole dihydrochloride, giving a white solid: yield 0.1 g (60%). The compound precipitated after reaction completion. The reaction mixture was filtered, and the residue was washed using petroleum ether (3 × 10 mL) to give the desired product; mp 239.7 °C; ^{1}H NMR (500 MHz, DMSO-d_6) δ 9.27 (t, J = 5.7 Hz, 1H), 8.04 (d, J = 0.6 Hz, 1H), 7.89 (d, J = 8.9 Hz, 1H), 7.42 (d, J = 2.4 Hz, 1H), 7.10 (dd, J = 8.9, 2.5 Hz, 1H), 6.93 (s, 2H), 4.50 (d, J = 5.7 Hz, 2H), 3.83 (s, 3H);

DOI: 10.1021/acs.jmedchem.6b01915
J. Med. Chem. XXXX, XXX, XXX−XXX

^{13}C NMR (126 MHz, DMSO-d_6) δ 161.60, 157.36, 144.55, 140.71, 140.66, 140.28, 132.69, 124.86, 123.54, 121.73, 116.72, 106.70, 55.38, 36.99; MS (ESI) m/z = 387.96 $(M + H)^+$. HRMS (ESI): calcd for ($C_{14}H_{14}N_3O_2S$) 288.08067, found 288.07992$(M + H)^+$. IR (cm^{-1}): $\tilde{\nu}$ 3288 (NH), 1629 (C═O).

Biological Assays. Protein Kinases and Inhibition Assays. Human Dyrk1A was expressed and purified as described earlier.[27] Active human Clk1 was purchased from Life Technologies (lot no. 1095729A, catalog no. PV3315). Woodtide substrate peptide for Dyrk1A (KKISGRLSPIMTEQ) and RS repeat substrate peptide for Clk1 (GRSRSRSRSRSRSR) were custom synthesized at the Department of Medical Biochemistry and Molecular Biology, Saarland University, Homburg, Germany. Kinase inhibition assays for Dyrk1A, Dyrk1B, Clk1, and CK2 were performed as described previously, in the presence of 15 μM ATP.[27] The calculated IC_{50} values are representative of at least two independent determinations. The larger panel of kinases shown in Table 3 was screened by the SelectScreen Kinase Profiling Service, Thermo Fisher Scientific, Paisley, U.K.

MTT Cell Growth Assay. The T24 bladder carcinoma cell line, the hepatocellular carcinoma cell line HepG2, and the breast cancer cell lines MDA-MB-231 and T47D were cultured in Dulbecco's modified Eagle medium (DMEM, Sigma-Aldrich). The acute monocytic leukemia cell line THP-1 and peripheral blood lymphocytes (PBLs, pooled samples from three healthy donors) were maintained in RPMI-1640 medium (Sigma-Aldrich). Both media were supplemented with 1% pen/strep solution (Invitrogen) and 5% fetal calf serum (FCS, Sigma-Aldrich). For the MTT assay, all cells except PBLs were seeded in a 96-well plate (5000 cells per well) already containing DMSO as a control (0.2% final concentration) or the test compounds dissolved in DMSO. The cells were grown for 5 days at 37 °C in a humidified incubator containing 5% CO_2, without further change of medium, before the detection was carried out as described.[28] PBLs were suspended in 96 well plates at 30 000 cells per well and maintained in the presence of compounds or DMSO for 2 days prior to measurement.

Treatment of Cell Lines and Immunoblotting Analysis. T24, MDA-MB-231, and HepG2 cells were seeded in Petri dishes (5.5 cm diameter) and grown to 70% confluency in DMEM medium as specified under "MTT Cell Growth Assay". The compounds were diluted from DMSO stocks in DMEM to the final concentrations indicated in the figure legend, and then the medium in the plates was exchanged by compound-containing medium. After 3 days in the incubator, the cells were washed once with phosphate buffered saline (PBS), harvested by the addition of 0.6 mL of 0.8× concentrated SDS-Laemmli buffer, and scraping off using a rubber cell scraper. The solution containing the lysed cells was concentrated to half the volume in a SpeedVac concentrator. For Western blot analysis, the high molecular weight DNA was sheared by passing the samples through a 23 gauge needle and syringe several times. Then the samples were separated by SDS−PAGE on 4−20% gradient gels (PAGEr Gels, Lonza) and then transferred to Immobilon FLPVDF membranes (Millipore), using a discontinuous buffer system in a semidry blotter (anode buffer, 60 mM Tris base, 40 mM *N*-cyclohexyl-3-aminopropanesulfonic acid (CAPS), pH 9.6, 15% methanol; cathode buffer, 60 mM Tris, 40 mM CAPS, 0.1% SDS). The membranes were blocked in blocking buffer (3% BSA in PBS) and incubated with suitable combinations of the following primary monoclonal antibodies in blocking buffer (all from Santa Cruz Biotechnology, dilutions all 1:660, antibody clone number in parentheses): EGFR (A-10), p70S6 kinase α (H-9), PARP-1 (F-2), ERK2 (D-2), HDAC1 (10E2), HCAM (=CD44) (DF1485), PCNA (PC10), GRP 94 (9G10) at 4 °C overnight. When the Clk1 protein expression was analyzed, total cell protein from untreated cells was harvested and subject to Western Blotting as above, and anti-Clk1/4 antibody (Santa Cruz Biotechnology catalog no. sc-515307, dilution 1:660) was applied. After incubation with the primary antibody, the membrane was washed four times using PBS with 0.1% Tween 20, incubated with the IRDye 680-conjugated anti-mouse IgG secondary antibody (diluted 1:10 000 in blocking buffer) for 1 h, and washed again four times as above. Finally the membrane was scanned using an Odyssey infrared imaging system (LI-COR). All cell treatments and immunoblotting analyses were performed two times in duplicates. The normalization of the signals according to the amount of loaded protein was performed in two ways: the gel used for the Western transfer was stained afterward using Coomassie blue, and the remaining protein bands quantified using GelQuant.NET software provided by biochemlabsolutions.com. In addition, the relative protein load was measured using signals from primary antibodies that were insensitive to the compound treatments.

Molecular Docking. All procedures were performed using the Molecular Operating Environment (MOE) software package (version 2010, Chemical Computing Group). For the docking simulations, PDB entries 1Z57 (Clk1 cocrystallized with hymenialdisine)[4] and 2WO6 (Dyrk1A cocrystallized with *N*-(5-1*H*-indazol-3-yl)benzamide) were used.[21] Molecular docking simulations with **21b** as a ligand were performed using the MMFF94x and OPLS-AA force fields and the "triangle matcher" method (number of return poses set to 2000) and "Force field" as refinement. The refinement setting was further configured as follows: free side chain movements enabled, cutoff 10 Å. By use of these settings, docking runs were performed in two different ways: (i) the binding pocket was defined by selecting residues Leu244, Lys191, and Gly173 (Clk1) or Leu241, Lys188, and Gly171 (Dyrk1A); (ii) after an initial run using condition (i), a pharmacophore was defined based on a suitable pose after energy minimization using the MOE LigX routine (settings: receptor strength = 1, ligand strength = 5000), by selecting both the methoxy oxygen close to the NH of the leucine and the carbonyl oxygen near the conserved lysine as acceptor points (this binding orientation prevailed among the poses with the compound docked deep in the pocket). In the pharmacophore definition window, the radius of the pharmacophore points was raised to 1.6 Å. The subsequent docking was performed using the pharmacophore-supported placement. The number of retained poses was set to 500 each time. Only the poses with the top 10 scoring values were further evaluated for plausibility. The final selected poses were optimized again using the LigX routine.

■ ASSOCIATED CONTENT

Supporting Information

The Supporting Information is available free of charge on the ACS Publications website at DOI: 10.1021/acs.jmedchem.6b01915.

Figures S1 and S2 (PDF)
Molecular formula strings (CSV)

■ AUTHOR INFORMATION

Corresponding Author

*Phone: +49 681 302 70312. Fax: +49 681 302 70308. E-mail: ma.engel@mx.uni-saarland.de.

ORCID

Mohammad Abdel-Halim: 0000-0003-1326-4219
Matthias Engel: 0000-0001-5065-8634

Author Contributions

The manuscript was written through contributions of all authors. All authors have given approval to the final version of the manuscript.

Notes

The authors declare no competing financial interest.

■ ACKNOWLEDGMENTS

We thank Prof. Dr. R. W. Hartmann and Prof. Dr. Christian Ducho for generously providing lab facilities to the M.E. group. A.K.E. and M.A.-H. acknowledge The Science & Technology Development Fund in Egypt (STDF) for funding through the GE-SEED, Project 17391. The support by the Deutsche Forschungsgemeinschaft (DFG) (Grant EN381/2-3) to M.E. is greatly acknowledged. The authors are particularly thankful to

DOI: 10.1021/acs.jmedchem.6b01915
J. Med. Chem. XXXX, XXX, XXX−XXX

Dr. Jessica Hoppstädter for her constant support and supply with reagents and cells.

■ ABBREVIATIONS USED

CC, column chromatography; CID, collision induced dissociation; Clk, cdc2-like kinase; CK, casein kinase; Dyrk, dual specificity protein kinase; GI_{50}, the concentration for 50% of maximal inhibition of cell proliferation; GRP94, glucose regulated protein 94; HBTU, *N*,*N*,*N*′,*N*′-tetramethyl-*O*-(1*H*-benzotriazol-1-yl)uronium hexafluorophosphate; HCAM, (=CD44) homing cell adhesion molecule; HIF, hypoxia inducible factor; HUVEC, human umbilical vein endothelial cell; KHMDS, potassium bis(trimethylsilyl)amide; MLCK2, myosin light chain kinase 2; MTT, 3-(4,5-dimethylthiazol-2-yl)-2,5-diphenyltetrazolium bromide; NFAT, nuclear factor of activated T-cell; NMD, nonsense-mediated decay; p70S6 kinase, ribosomal protein S6 kinase; PARP-1, poly ADP ribose polymerase 1; PCNA, proliferating cell nuclear antigen; SPF45, splicing factor 45; STK17, serine threonine kinase 17

■ REFERENCES

(1) Duncan, P. I.; Stojdl, D. F.; Marius, R. M.; Scheit, K. H.; Bell, J. C. The Clk2 and Clk3 dual-specificity protein kinases regulate the intranuclear distribution of SR proteins and influence pre-mRNA splicing. *Exp. Cell Res.* **1998**, *241*, 300−308.

(2) Menegay, H.; Moeslein, F.; Landreth, G. The dual specificity protein kinase CLK3 is abundantly expressed in mature mouse spermatozoa. *Exp. Cell Res.* **1999**, *253*, 463−473.

(3) Wong, R.; Balachandran, A.; Mao, A. Y.; Dobson, W.; Gray-Owen, S.; Cochrane, A. Differential effect of CLK SR kinases on HIV-1 gene expression: potential novel targets for therapy. *Retrovirology* **2011**, *8*, 47.

(4) Bullock, A. N.; Das, S.; Debreczeni, J. E.; Rellos, P.; Fedorov, O.; Niesen, F. H.; Guo, K.; Papagrigoriou, E.; Amos, A. L.; Cho, S.; Turk, B. E.; Ghosh, G.; Knapp, S. Kinase domain insertions define distinct roles of CLK kinases in SR protein phosphorylation. *Structure* **2009**, *17*, 352−362.

(5) Colwill, K.; Feng, L. L.; Yeakley, J. M.; Gish, G. D.; Cáceres, J. F.; Pawson, T.; Fu, X. D. SRPK1 and Clk/Sty protein kinases show distinct substrate specificities for serine/arginine-rich splicing factors. *J. Biol. Chem.* **1996**, *271*, 24569−24575.

(6) Eisenreich, A.; Bogdanov, V. Y.; Zakrzewicz, A.; Pries, A.; Antoniak, S.; Poller, W.; Schultheiss, H. P.; Rauch, U. Cdc2-like kinases and DNA topoisomerase I regulate alternative splicing of tissue factor in human endothelial cells. *Circ. Res.* **2009**, *104*, 589−599.

(7) Liu, Y.; Conaway, L.; Rutherford Bethard, J.; Al-Ayoubi, A. M.; Thompson Bradley, A.; Zheng, H.; Weed, S. A.; Eblen, S. T. Phosphorylation of the alternative mRNA splicing factor 45 (SPF45) by Clk1 regulates its splice site utilization, cell migration and invasion. *Nucleic Acids Res.* **2013**, *41*, 4949−4962.

(8) Araki, S.; Dairiki, R.; Nakayama, Y.; Murai, A.; Miyashita, R.; Iwatani, M.; Nomura, T.; Nakanishi, O. Inhibitors of CLK protein kinases suppress cell growth and induce apoptosis by modulating pre-mRNA splicing. *PLoS One* **2015**, *10*, e0116929.

(9) Jakubauskiene, E.; Vilys, L.; Makino, Y.; Poellinger, L.; Kanopka, A. Increased serine-arginine (SR) protein phosphorylation changes pre-mRNA splicing in hypoxia. *J. Biol. Chem.* **2015**, *290*, 18079−18089.

(10) Eisenreich, A.; Zakrzewicz, A.; Huber, K.; Thierbach, H.; Pepke, W.; Goldin-Lang, P.; Schultheiss, H. P.; Pries, A.; Rauch, U. Regulation of pro-angiogenic tissue factor expression in hypoxia-induced human lung cancer cells. *Oncol. Rep.* **2013**, *30*, 462−470.

(11) Capra, M.; Nuciforo, P. G.; Confalonieri, S.; Quarto, M.; Bianchi, M.; Nebuloni, M.; Boldorini, R.; Pallotti, F.; Viale, G.; Gishizky, M. L.; Draetta, G. F.; Di Fiore, P. P. Frequent alterations in the expression of serine/threonine kinases in human cancers. *Cancer Res.* **2006**, *66*, 8147−8154.

(12) Yoshida, T.; Kim, J. H.; Carver, K.; Su, Y.; Weremowicz, S.; Mulvey, L.; Yamamoto, S.; Brennan, C.; Mei, S.; Long, H.; Yao, J.; Polyak, K. CLK2 is an oncogenic kinase and splicing regulator in breast cancer. *Cancer Res.* **2015**, *75*, 1516−1526.

(13) Muraki, M.; Ohkawara, B.; Hosoya, T.; Onogi, H.; Koizumi, J.; Koizumi, T.; Sumi, K.; Yomoda, J.; Murray, M. V.; Kimura, H.; Furuichi, K.; Shibuya, H.; Krainer, A. R.; Suzuki, M.; Hagiwara, M. Manipulation of alternative splicing by a newly developed inhibitor of Clks. *J. Biol. Chem.* **2004**, *279*, 24246−24254.

(14) Fedorov, O.; Huber, K.; Eisenreich, A.; Filippakopoulos, P.; King, O.; Bullock, A. N.; Szklarczyk, D.; Jensen, L. J.; Fabbro, D.; Trappe, J.; Rauch, U.; Bracher, F.; Knapp, S. Specific CLK inhibitors from a novel chemotype for regulation of alternative splicing. *Chem. Biol.* **2011**, *18*, 67−76.

(15) Mott, B. T.; Tanega, C.; Shen, M.; Maloney, D. J.; Shinn, P.; Leister, W.; Marugan, J. J.; Inglese, J.; Austin, C. P.; Misteli, T.; Auld, D. S.; Thomas, C. J. Evaluation of substituted 6-arylquinazolin-4-amines as potent and selective inhibitors of cdc2-like kinases (Clk). *Bioorg. Med. Chem. Lett.* **2009**, *19*, 6700−6705.

(16) Gao, Y.; Davies, S. P.; Augustin, M.; Woodward, A.; Patel, U. A.; Kovelman, R.; Harvey, K. J. A broad activity screen in support of a chemogenomic map for kinase signalling research and drug discovery. *Biochem. J.* **2013**, *451*, 313−328.

(17) Schmitt, C.; Miralinaghi, P.; Mariano, M.; Hartmann, R. W.; Engel, M. Hydroxybenzothiophene ketones are efficient pre-mRNA splicing modulators due to dual inhibition of Dyrk1A and Clk1/4. *ACS Med. Chem. Lett.* **2014**, *5*, 963−907.

(18) Kuhn, C.; Frank, D.; Will, R.; Jaschinski, C.; Frauen, R.; Katus, H. A.; Frey, N. DYRK1A is a novel negative regulator of cardiomyocyte hypertrophy. *J. Biol. Chem.* **2009**, *284*, 17320−17327.

(19) Bendjeddou, L. Z.; Loaëc, N.; Villiers, B.; Prina, E.; Späth, G. F.; Galons, H.; Meijer, L.; Oumata, N. Exploration of the imidazo[1,2-b]pyridazine scaffold as a protein kinase inhibitor. *Eur. J. Med. Chem.* **2017**, *125*, 696−709.

(20) Prak, K.; Kriston-Vizi, J.; Chan, A. W.; Luft, C.; Costa, J. R.; Pengo, N.; Ketteler, R. Benzobisthiazoles represent a novel scaffold for kinase inhibitors of CLK family members. *Biochemistry* **2016**, *55*, 608−617.

(21) Soundararajan, M.; Roos, A. K.; Savitsky, P.; Filippakopoulos, P.; Kettenbach, A. N.; Olsen, J. V.; Gerber, S. A.; Eswaran, J.; Knapp, S.; Elkins, J. M. Structures of down syndrome kinases, DYRKs, reveal mechanisms of kinase activation and substrate recognition. *Structure* **2013**, *21*, 986−996.

(22) Paulini, R.; Müller, K.; Diederich, F. Orthogonal multipolar interactions in structural chemistry and biology. *Angew. Chem., Int. Ed.* **2005**, *44*, 1788−1805.

(23) Olsen, J. A.; Banner, D. W.; Seiler, P.; Obst Sander, U.; D'Arcy, A.; Stihle, M.; Müller, K.; Diederich, F. A fluorine scan of thrombin inhibitors to map the fluorophilicity/fluorophobicity of an enzyme active site: evidence for C-F...C=O interactions. *Angew. Chem., Int. Ed.* **2003**, *42*, 2507−2511.

(24) Ogawa, Y.; Nonaka, Y.; Goto, T.; Ohnishi, E.; Hiramatsu, T.; Kii, I.; Yoshida, M.; Ikura, T.; Onogi, H.; Shibuya, H.; Hosoya, T.; Ito, N.; Hagiwara, M. Development of a novel selective inhibitor of the down syndrome-related kinase Dyrk1A. *Nat. Commun.* **2010**, *1*, 86.

(25) Okano, J.; Nagahara, T.; Matsumoto, K.; Murawaki, Y. Caffeine inhibits the proliferation of liver cancer cells and activates the MEK/ERK/EGFR signalling pathway. *Basic Clin. Pharmacol. Toxicol.* **2008**, *102*, 543−551.

(26) Sakuma, M.; Iida, K.; Hagiwara, M. Deciphering targeting rules of splicing modulator compounds: case of TG003. *BMC Mol. Biol.* **2015**, *16*, 16.

(27) Schmitt, C.; Kail, D.; Mariano, M.; Empting, M.; Weber, N.; Paul, T.; Hartmann, R. W.; Engel, M. Design and synthesis of a library of lead-like 2,4-bisheterocyclic substituted thiophenes as selective Dyrk/Clk inhibitors. *PLoS One* **2014**, *9*, e87851.

(28) Mariano, M.; Hartmann, R. W.; Engel, M. Systematic diversification of benzylidene heterocycles yields novel inhibitor

DOI: 10.1021/acs.jmedchem.6b01915
J. Med. Chem. XXXX, XXX, XXX−XXX

scaffolds selective for Dyrk1A, Clk1 and CK2. *Eur. J. Med. Chem.* **2016**, *112*, 209−216.
(29) Tahtouh, T.; Elkins, J. M.; Filippakopoulos, P.; Soundararajan, M.; Burgy, G.; Durieu, E.; Cochet, C.; Schmid, R. S.; Lo, D. C.; Delhommel, F.; Oberholzer, A. E.; Pearl, L. H.; Carreaux, F.; Bazureau, J. P.; Knapp, S.; Meijer, L. Selectivity, cocrystal structures, and neuroprotective properties of leucettines, a family of protein kinase inhibitors derived from the marine sponge alkaloid leucettamine B. *J. Med. Chem.* **2012**, *55*, 9312−9330.
(30) Bain, J.; McLauchlan, H.; Elliott, M.; Cohen, P. The specificities of protein kinase inhibitors: an update. *Biochem. J.* **2003**, *371*, 199−204.
(31) Anastassiadis, T.; Deacon, S. W.; Devarajan, K.; Ma, H.; Peterson, J. R. Comprehensive assay of kinase catalytic activity reveals features of kinase inhibitor selectivity. *Nat. Biotechnol.* **2011**, *29*, 1039−1045.
(32) Cuny, G. D.; Robin, M.; Ulyanova, N. P.; Patnaik, D.; Pique, V.; Casano, G.; Liu, J. F.; Lin, X.; Xian, J.; Glicksman, M. A.; Stein, R. L.; Higgins, J. M. Structure-activity relationship study of acridine analogs as haspin and DYRK2 kinase inhibitors. *Bioorg. Med. Chem. Lett.* **2010**, *20*, 3491−3494.

DOI: 10.1021/acs.jmedchem.6b01915
J. Med. Chem. XXXX, XXX, XXX−XXX